Journal of Materials Research and Technology 31 (2024) 971–997

Contents lists available at ScienceDirect

Journal of Materials Research and Technology

journal homepage: www.elsevier.com/locate/jmrt

Prospects of friction stir processed Mg alloys and composites-Reviews and suggestions

K. Palanikumar [a], Elango Natarajan [b,*], S. Suresh [c], Dhanesh G. Mohan [d], Chander Prakash [e], Kirtanjot Kaur [f]

[a] Department of Mechanical Engineering, Sri Sai Ram Institute of Technology, Chennai, India
[b] Faculty of Engineering, Technology and Built Environment, UCSI University, Kuala Lumpur, Malaysia
[c] Department of Mechanical Engineering, Erode Sengunthar Engineering College, Erode, Tamilnadu, India
[d] School of Engineering, Faculty of Technology, University of Sunderland, Sunderland, United Kingdom
[e] University Centre for Research and Development, Chandigarh University, Mohali, Punjab, 140413, India
[f] University Centre for Research and Development, Chandigarh University, Mohali, 140413, India

ARTICLE INFO

Handling editor: SN Monteiro

Keywords:
FSP
Submerged FSP
Cryogenic-cooling FSP
Magnesium alloy
Sustainable manufacturing
Additive manufacturing
Product Innovation

ABSTRACT

The pursuit of advanced materials with enhanced or tailored properties has indeed been a crucial focus in various industries. From aerospace to automotive, and from nuclear power to space exploration, the need for materials that can withstand extreme conditions, offer improved performance, and ensure safety is paramount. Safety standards are vital in industries where materials are subjected to extreme conditions or where failure could have catastrophic consequences. Therefore, research in advanced materials not only focuses on enhancing properties but also ensuring that these materials meet rigorous safety standards. Friction stir processing (FSP) emerges as a transformative methodology, facilitating the achievement of superplasticity, enhanced ductility, heightened strength, toughness, and hardness, all while preserving the structural integrity of the material. In recent years, notable advancements have been witnessed in preparing magnesium (Mg) alloys, Mg composites, and functional Mg materials. This comprehensive review encompasses the latest developments, global significance, adherence to standards, and innovative strides in Mg alloys from 2011 to 2023. It includes the FSP processing techniques, governing mechanism, advantageous properties, grain size, dislocations and their impacts, corrosion, wear behaviour, formability studies, cryogenic FSP, underwater FSP and friction stir additive manufacturing. Readers will gain critical insights, receive constructive suggestions, and discern future directions from this extensive review, as it encapsulates the trajectory of advancements in Mg alloys and delineates promising horizons with potentially transformative impacts in materials science research. Prospects and potential areas would deem help upcoming researchers to pursue with new advanced materials.

1. Introduction

Mg and its alloys, distinguished from steel and Aluminium (Al) by a density of 78% and 40% lower respectively, have emerged as compelling alternatives for steel and Al alloys. Mg alloys exhibit a harmonious amalgamation of qualities, including comparable strength, an impressive weight-to-strength ratio, facile castability, efficient machinability, exceptional formability, recyclability, pronounced damping characteristics, and a notable weight-to-stiffness ratio, positioning them as formidable contenders to displace Al alloys across a broad spectrum of industrial applications [1–4]. Spanning a historical timeline of two centuries, the evolution of Mg alloys unveils four distinct phases: an initial 80-year period of laboratory testing, followed by a 40-year phase of semi-technical expansion, succeeded by 30 years of robust commercial and industrial utilization, culminating in their diverse deployment across fields encompassing medicine, industry, and scientific technology, albeit with inherent challenges [5]. China, a dominant player, spearheads the global supply chain of Mg alloys, profoundly influencing the material's market dynamics [6,7]. Illustrated in Fig. 1, a comprehensive array of fabrication processes encapsulates the manufacturing of Mg alloys and Mg metal matrix composites, reflecting their versatility and adaptability to various application demands. In summation, the

* Corresponding author.
E-mail address: elango@ucsiuniversity.edu.my (E. Natarajan).

https://doi.org/10.1016/j.jmrt.2024.06.087
Received 20 February 2024; Received in revised form 6 June 2024; Accepted 12 June 2024
Available online 14 June 2024

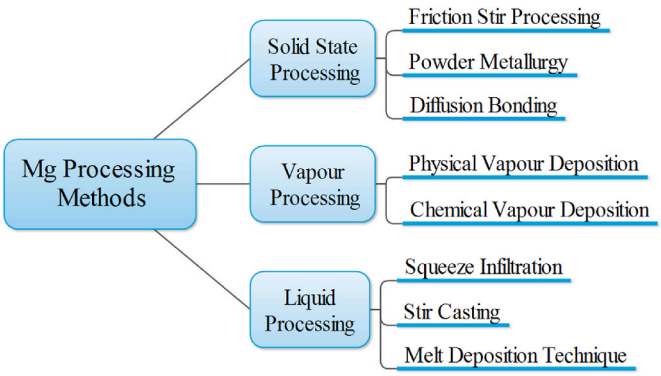

Fig. 1. Mg alloys/composites fabrication processes.

trajectory of Mg alloys as compelling substitutes is underscored by their distinctive properties, historical progression, and burgeoning integration into the industry, poised to reshape material engineering guided by their exceptional attributes and China's strategic role in shaping their global prominence.

Mg alloys have garnered widespread utilization across diverse industrial sectors, serving as indispensable components in various applications. These applications encompass a broad spectrum, ranging from brackets for braking and clutch systems [8], transmission housing, landing gear for aircraft [9], rotor fittings in helicopter, gearbox enclosure, high-speed textile machinery [10], commercial luggage, hand tools, computer casings, and ladders [11]. Mg alloys and composites have found a niche in electronics, contributing to the production of housing and packaging, hard disk arms, and cell phones. The rationale for adopting Mg alloys over plastics is their exceptional endurance strength and low density, rendering them conducive to dynamic loading conditions [12,13]. Moreover, these alloys offer superior heat dissipation, electromagnetic shielding, and minimal radio frequency interference [14]. Notably, Mg alloys extend their impact to biomedical applications, encompassing cardiovascular stents, orthopedic devices, and wheelchairs, underpinned by their commendable biocompatibility and absorbability [15,16]. However, challenges persist, encompassing and discharging capacities alongside a heightened degradation rate [17]. Despite making inroads into vehicular applications such as Jeep, Mercedes-Benz, Ford light trucks, and Renault 18 Turbo vehicles limitations in strength and plasticity hinder the broader integration of Mg alloys in large-scale contexts [18]. To surmount these challenges, surface coatings enhance strength, plasticity, and corrosion resistance, enabling them to compete with traditional materials effectively.

Table 1 provides a comprehensive compilation of published ISO standards pertaining to Mg and its alloys since 1972, encapsulating the evolving regulatory landscape of this material.

The pursuit of enhancing material properties finds realization through meticulous surface modification techniques, including high-energy laser beam irradiation, spraying, cast sintering, laser melt injection, electron beam irradiation, and innovative FSP [19–22]. The methodologies aforementioned, excluding FSP, constitute liquid-state processing methods executed at elevated temperatures. However, their effectiveness is curtailed by two primary limitations: (a) the intricate control of process parameters (b) the formation of detrimental surface states due to suboptimal interfacial reactions between the matrix and reinforcing components. Addressing these concerns, FSP emerges as a compelling alternative characterized by solid-state processing principles that prevent the challenges associated with liquid-state techniques [23–25]. FSP orchestrates the continuous agitation of hard particulates or reinforcing materials across the substrate, generating significant thermal energy that engenders transformative structural modifications within the substrate. A mature solid-state welding technique, involves temperature, mechanics, metallurgy and interactions [26], and severe

Table 1
ISO standards-Mg and Mg alloys (1972–2021).

Standard	Description	Publication Year
ISO 23700:2021	Rolled Plate and sheets – Wrought Mg and Mg alloy (ed.1)	March 2021
ISO 8287:2021	Chemical composition - Mg and Mg alloy, Unalloyed Mg (ed.4)	June 2021
ISO23694:2021	Wrought Mg and Mg alloy alloy-Espoused Rods/Bars and tubes	January 2021
ISO 26202:2019	Cast anodes of Mg and Mg alloys (ed.2)	October 2019
ISO 20260:2019	Determination of mercury - Mg and Mg alloy	July 2019
ISO 3116:2019	Wrought Mg and Mg alloys (ed.5)	May 2019
ISO 20258:2018	Determination of lithium - Inductively coupled plasma optical emission spectrometric method- Mg-Lithium alloys.	August 2018
ISO 16220:2017	Mg alloy ingots and castings (ed.3)	August 2017
ISO 16374:2016	Evaluation method for cleanliness of Mg and Mg alloy ingots(ed.1)	January 2016
ISO 10204:2015	Determination of Mg in Iron ores-Flame atomic absorption spectrometric method (ed.3)	August 2015
ISO 17403:2014	Determination of Mg of field and concentrated natural rubber latices by titration method (cyanide-free method) (ed.1)	March 2014
ISO 13933:2014	Determination of calcium and Mg in Steel and Iron- Inductively coupled plasma atomic emission spectrometric method (ed.1)	July 2014
ISO 23079:2013	Mg and Mg alloy-returns-requirements, classification and acceptance	December 2013
ISO 8287:2011	Unalloyed Mg - Mg and Mg alloy–Chemical composition	November 2011
ISO 11707:2011	Determination of lead and cadmium- Mg and Mg alloy	August 2011
ISO 11852:2011	Determination of Mg content of field and concentrated natural rubber latex by titration method (ed.1)	November 2011
ISO 11876:2010	Determination of calcium, copper, iron, potassium, Mg, manganese, sodium, nickel and zinc in cobalt metal powders-Flame atomic absorption spectrometric method (ed.1)	August 2010
ISO 27085:2009	Determination of calcium, sodium, phosphorus, Mg, potassium, iron, zinc, copper, manganese, cobalt, molybdenum, arsenic, lead and cadmium by ICP-AES – Animal feeding stuffs (ed.1)	April 2009
ISO 26202:2007	Cast anodes of Mg and Mg alloy (ed.1)	September 2007
ISO 3116:2007	Wrought Mg alloys (ed.4)	April 2007
ISO 21869:2006	Rubber compounding ingredients-Mg oxide-methods of test (ed.1)	April 2006
ISO 3750:2006	Determination of Mg content-Flame atomic absorption spectrometric method – Zn alloys	June 2006
ISO 10204:2006	Determination of Mg-Flame atomic absorption spectrometric method- Iron ores (ed.2)	June 2006
ISO 23079:2005	Mg and Mg alloy-Returns-Requirements, classification and acceptance (ed.1)	March 2005
ISO 16220:2005	Ingots and castings of Mg and Mg alloy	March 2005
ISO 16220:2002	Ingots and castings of Mg and Mg alloy	February 2002
ISO 6233:2001	Determination of calcium and Mg contents in Manganese ores and concentrates- EDTA titrimetric method	June 2001
ISO 7980:1997	Determination of calcium and Mg-Atomic absorption spectrometric method- water quality	January 1997
ISO 1178:1976	Determination of soluble Zr-Alizarin sulphonate photometric method (ed.2)	March 1976
ISO 794:1976	Determination of copper content-Oxalyldihydrazide photometric method	February 1976
ISO 121:1995	Mg–Al–Zn alloy ingots and alloy castings-Chemical composition and mechanical properties of sand cast reference test bars	February 1995
ISO101363:1993	Analysis of extract solutions-Part 3: Determination of calcium oxide and Mg oxide	July 1993

(*continued on next page*)

Table 1 (*continued*)

Standard	Description	Publication Year
	by flame atomic absorption spectrometry (ed.1) – Glass and Glassware	
ISO 9916:1991	Liquid penetrant inspection (ed.1) -Al alloy and Mg alloy castings	February 1991
ISO 9668:1990	Determination of Mg content-Flame atomic absorption spectrometric method (ed.1) -Pulps	February 1990
ISO 7980:1986	Determination of calcium and Mg-Atomic absorption spectrometric method (ed.1) -Water quality	May 1986
ISO 7953:1985	Determination of calcium and Mg contents-Flame atomic absorption spectrometric method-Manganese ores and concentrates	December 1985
ISO 5399:1984	Determination of water-soluble Mg salts — EDTA titrimetric method(ed.1) - Leather	February 1984
ISO 7773:1983	Mg alloys round bars and tubes-Dimensional tolerances(ed.1)	August 1983
ISO 2107:1983	Al–Mg and their alloys-Temper designations (ed.1)	June 1983
ISO 4194:1981	Determination of zinc content – Flame atomic absorption spectrometric method(ed.1) – Mg alloys	January 1981
ISO 7242:1981	Chemical analysis of light metals and their alloys – Statistical interpretation of inter-laboratory trials (ed.1)	January 1981
ISO51962:1980	Mg alloys-Determination of thorium-Part 2: Titrimetric method	January 1980
ISO51961:1980	Mg alloys-Determination of thorium-Part 1: Gravimetric method	January 1980
ISO 4058:1977	Determination of nickel-Photometric method using dimethylglyoxime - Mg and Mg alloy	September 1977
ISO 3335:1977	Extruded solid profiles in Al-zinc- Mg alloy Al Zn4,5 Mg1 (7020) — Chemical composition and mechanical properties (ed.1)	December 1977
ISO 3256:1977	Determination of Mg in Al and Al alloys-Atomic absorption spectrophotometric method (ed.1)	May 1977
ISO 794:1976	Determination of copper content-Oxalyldihydrazide photometric method(ed.1) - Mg and Mg alloy	February 1976
ISO 2354:1976	Determination of insoluble zirconium-Alizarin sulphonate photometric method (ed.2) – Mg alloys	April 1976
ISO 3255:1974	Determination of Al – Chromazurol S photometric method - Mg and Mg alloy	August 1974
ISO 791:1973	Determination of Al-hydroxyquinoline gravimetric method (ed.1) - Mg and Mg alloy	January 1973
ISO 809:1973	Determination of manganese-Periodate photometric method(Manganese content between 0.01 and 0.8%)(ed.1)	January 1973
ISO 810:1973	Determination of manganese-Periodate photometric method(Manganese content less than 0.01%)(ed.1)	January 1973
ISO 1975:1973	Determination of silicon – Spectrophotometric method with the reduced silico-molybdic complex (ed.1)	January 1973
ISO 1783:1973	Determination of zinc-Volumetric method	January 1973
ISO 2355:1972	Determination of rare earths – Chemical analysis of Mg and Mg alloy-Gravimetric method (ed.1)	January 1972

plastic deformation and corresponding frictional/deformation heat contributed to solid-state and microstructural modification has inhibited the growth of recrystallized grains effectively to obtain fine-grain microstructures [27].

In alignment with this objective, this review article explores recent advancements in friction stir processed Mg alloys. This comprehensive analysis delves into multifaceted dimensions, encompassing mechanical and metallurgical enhancements, wear behavior elucidation and correction, deformation responses, the influence of distinct cooling conditions ranging from underwater to cryogenic settings and the augmentative potential of additive FSP techniques. By elucidating the evolving landscape of FSP applied to Mg alloys, this review contributes to an enriched understanding of the potentiality and its pertinent implications across diverse applications.

2. Overview of friction stir processes and their effectiveness

This section provides a comprehensive exposition of the friction FSP methodologies and their profound efficacy in effecting surface modifications within the substrate. Fig. 2 visually delineates the FSP process, an evolutionary offshoot derived from friction stir welding (FSW). Employing a non-consumable, revolving tool comprised of a pin and shoulder, the FSP method intricately embeds itself within the workpiece, meticulously refining surface grains while preserving the underlying substrate phase [28,29]. The mechanism underpinning this process relies on generating elevated frictional heat and localized plasticity within the material, culminating in a consequential enhancement of material properties. Supplementary advancements manifest by strategically introducing reinforcing materials, such as SiC, Alumina, and TiB_2 [30]. When judiciously inserted within grooves or holes, these reinforcing elements solidify within the FSPed region, synergistically intermingling with the substrate's grain structure as the tool transverses [31,32]. Fig. 3 visually illustrates the preparation of a friction stir composite replete with fillers. Notably, this process aligns with the principles of green manufacturing, circumventing concerns associated with arc flash, emissions, and dispersion.

The realization of improved material properties hinges upon attaining uniform and equiaxed grain distribution across the surface. This intricate balance is intricately governed by a constellation of factors, wherein the geometrical parameters of the tool and the intricacies of the processing regimen take center stage. Rotational speed, feed rate, tool geometry, number of passes, groove design, and filler material collectively compose the repertoire of process parameters [29,34–36]. Conversely, the probe's shape, dimensions, shoulder configuration, and diameter encompass the geometrical properties integral to the process. These parameters collectively orchestrate localized plastic flow, grain refinement, and consequential alterations in material properties [37–40]. This ventures forth by delving into the nuanced interplay between process parameters and tool geometry, dissecting their impacts on the overall FSP methodology.

The efficacy of FSP is contingent upon a triad of influential factors, encompassing tool-related parameters, machine-related parameters, and material-related parameters. Central to the friction stir tool's operation are two pivotal components the pin and the shoulder both integral in engendering frictional heat and facilitating localized plastic deformation within the material. Notably, the shoulder assumes a dual role, serving as both the source of frictional heat generation and the mechanism for imparting pressure onto the substrate [41–43]. For a comprehensive depiction of the interplay between FSP process parameters, refer to Fig. 4, which elucidates a cause-and-effect diagram.

The stirring tool's significance in FSP, particularly concerning Mg alloys composites, cannot be overstated. In the realm of Mg alloys composites, the choice of stirring tool design and material becomes even more critical due to the inherent characteristics of Mg-based materials. Mg alloys are known for their lightweight properties, high specific strength, and excellent machinability, making them desirable for various applications, including aerospace, automotive, and biomedical industries [44]. However, they also pose specific challenges during processing, such as low thermal conductivity, high reactivity with oxygen, and tendency to form brittle intermetallic phases. To effectively address these challenges in Mg alloys composites, stirring tool designs are tailored to promote efficient material flow, minimize thermal effects, and mitigate the formation of detrimental intermetallic compounds. Various tool configurations, such as specialized pin geometries and shoulder profiles, are optimized to facilitate uniform plastic deformation and grain refinement in Mg alloys composites [45,46]. Moreover, the selection of tooling materials is carefully curated to withstand the

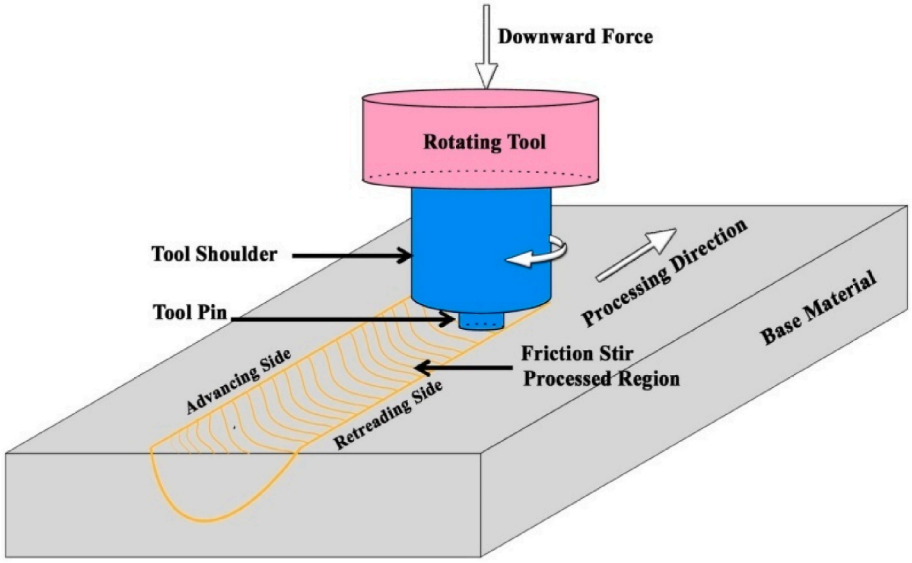

Fig. 2. Schematic illustration of the FSP technique.

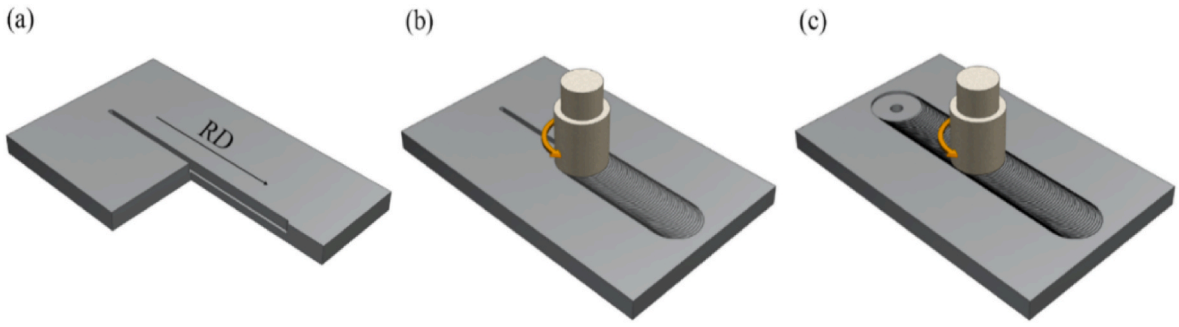

Fig. 3. Friction stir composite: (a) sectional view of pre-grooved plate (b) closing the groove using a pin less tool (c) processing using a tool with a pin [33].

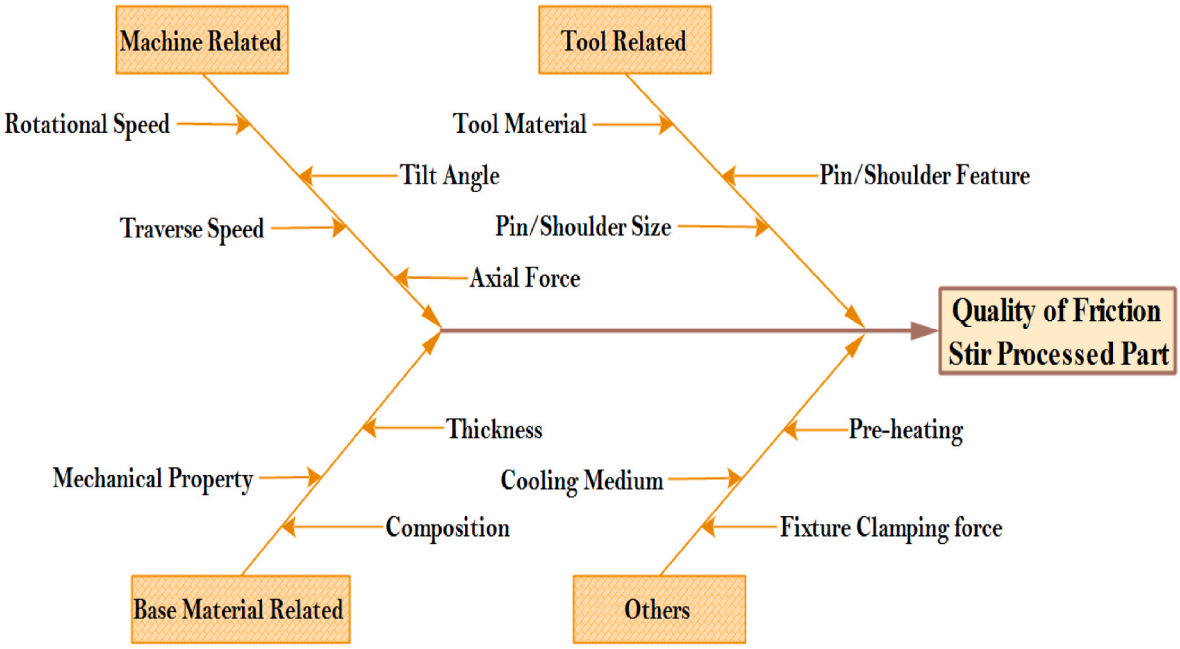

Fig. 4. Cause and effect diagram of FSP process parameters.

unique demands imposed by Mg alloys composites. While H13 steel remains a preferred choice for its robustness and versatility, researchers also explore alternative materials with enhanced wear resistance and thermal stability, specifically tailored for processing Mg alloys composites [47–49]. Notably, to reinforce the tool's robustness, a selection of hard materials has been harnessed. Poly-cubic boron nitride (PCBN), tungsten carbide (WC), cobalt (Co) alloys, SiC, Alumina and cermets are some materials attempted on this topic of research.

For a comprehensive overview of diverse FSP tool profiles, refer to Fig. 5. In the context of FSP, the synergistic interplay of the aggressive stir action imparted by the FSP tool, along with the ensuing severe plastic deformation of the material, culminates in the development of a composite layer spanning the range of 0.1–6 mm.

The FSP procedure yields discernible microstructure zones within the substrate, as delineated in Fig. 6. The stir zone (SZ), synonymous with the tool probe region, exhibits a distinctive recrystallized grain structure resulting from the dual effects of intense deformation and frictional heat. Termed the Nugget zone, this region boasts finely equiaxed recrystallized grains alongside sub-grain boundaries. The thermo-mechanically affected zone (TMAZ) is proximate to the nugget zone, characterized by a dominant influence of dissipated heat and consequential plastic deformation. Adjacent to the TMAZ, the heat affected zone (HAZ) materializes as a consequence of the thermal cycle, devoid of significant plastic deformation. This zone manifests larger grain sizes compared to the substrate [50].

Based on the characteristics of the FSP process, several inherent issues arise, leading to defects in the processed area. These defects can significantly affect the mechanical properties and integrity of the processed surface. Here are the three main issues and potential solutions.

- Voids/Porosity: Voids or porosity can occur in the processed material due to insufficient material flow or entrapment of gas bubbles during the stirring process. This defect can weaken the material and reduce its mechanical properties. Optimization of process parameters such as rotation speed, traverse speed, and tool geometry can help improve material flow and minimize the formation of voids. Additionally, vacuum or inert gas environments can be employed to reduce gas entrapment [52].
- Surface irregularities: Irregularities on the surface of the processed material, such as ripples or groove-like patterns, may occur due to improper tool geometry or inadequate control over process parameters. Selecting an appropriate tool design with optimal shoulder and pin dimensions, along with precise control of process parameters, can help minimize surface irregularities. Adjustments in tool traverse speed and tool tilt angle can also contribute to achieving a smoother surface finish [53,54].
- Thermal damage: Excessive heat generation during FSP can lead to thermal damage in the form of grain growth, softening, or even localized melting, especially in heat-sensitive materials [55]. Implementing effective cooling strategies, such as using chilled backing plates or applying cryogenic cooling techniques, can help control the temperature rise and mitigate thermal damage. Furthermore, reducing the processing temperature or employing multi-pass processing can help distribute heat more uniformly and minimize thermal effects [56,57].

Various methodologies are employed within the ambit of FSP, encompassing friction stir surface cladding (FSSC), friction stir composites, ultrasonic-assisted FSP, multi-pass FSP, friction stir extrusion (FSE), and FSP additive manufacturing technology, as delineated in the literature [58]. A novel technique, FSSC has emerged, drawing inspiration from FSP principles, with its primary objective being the deposition of thin-clad material layers onto substrates [59]. Composites that undergo surface modification via FSP are classified as friction stir composites, with this approach currently applied to both ex-situ and in-situ nanocomposites [60,61]. In pursuit of enhanced microstructural refinement and elevated mechanical properties, ultrasonic energy can be judiciously introduced into the stir zone, a methodology referred to as ultrasonic vibration-assisted FSP, exemplified in Fig. 7 [62,63].

The technology involves a tool laden with reinforcement material and fillers, which, upon dispersion, culminate in forming a composite film on the substrate. The implementation of multiple or sequential passes has been considered to achieve finer structural attributes. In cases of overlapping passes, each travel witnesses full or partial interpenetration of stirring, resulting in the uniform thickness formation of a composite layer featuring homogenized ultra-fine grain dimensions [64]. The distinct stages of FSP overlap are portrayed in Fig. 8 [65].

FSE, constituting another solid-state process, amalgamates mechanical and thermo-mechanical processing within a singular step [66], as illustrated in Fig. 9. Baffari et al. [67] have underscored the potential utility of this approach in the production of Mg alloys.

Venturing into innovative terrain, submerged FSP, as depicted in Fig. 10, orchestrates severe plastic deformation upon a sample immersed in liquid, culminating in enhanced fine grain attributes and correspondingly augmented material strength [68]. Cryogenic friction stir processing (CFSP) introduces a cryogenic (LN2) element during FSP, as elucidated in Fig. 11, manifesting a unique avenue of exploration [69].

3. Published research on FSP of Mg alloys and composites

Within this section, a comprehensive presentation and discourse are undertaken regarding the outcomes encapsulating properties, microstructural analysis, corrosion rate, wear characteristics, and super

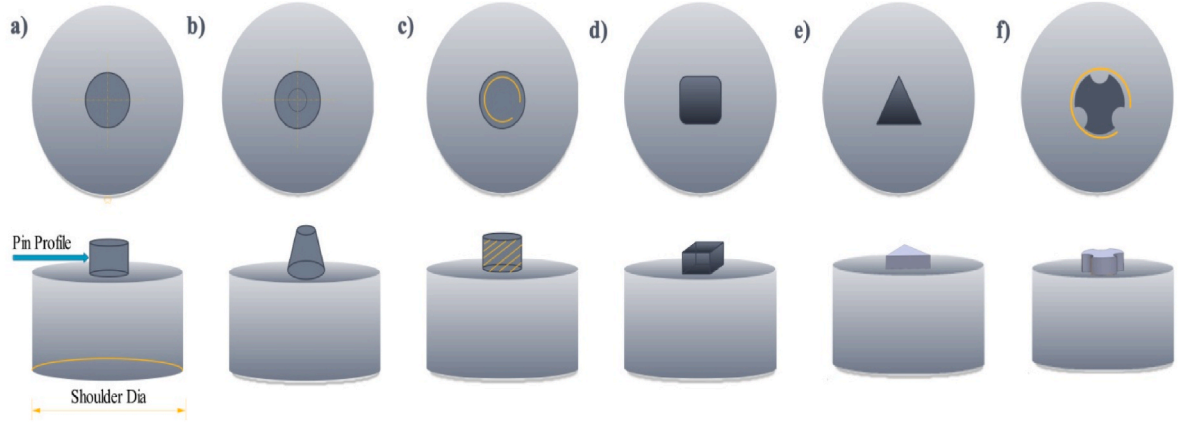

Fig. 5. FSP tool pin profiles a) Cylindrical b) Conical c) Threaded cylindrical d) Square e) Triangular and f) Threaded cylindrical flutes.

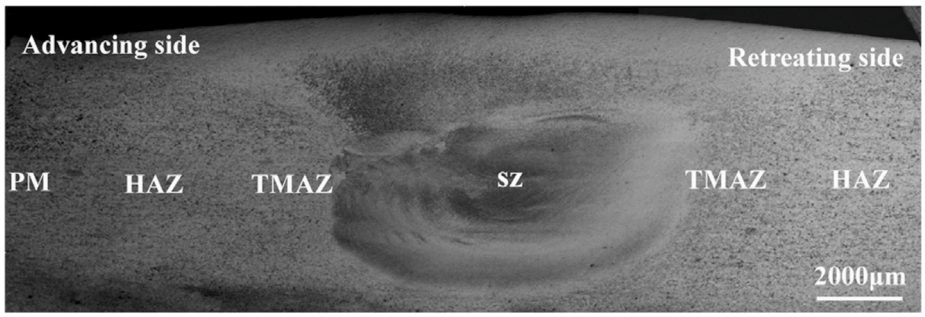

Fig. 6. Typical cross-sectional OM images showing various zones of FSPed sample [51].

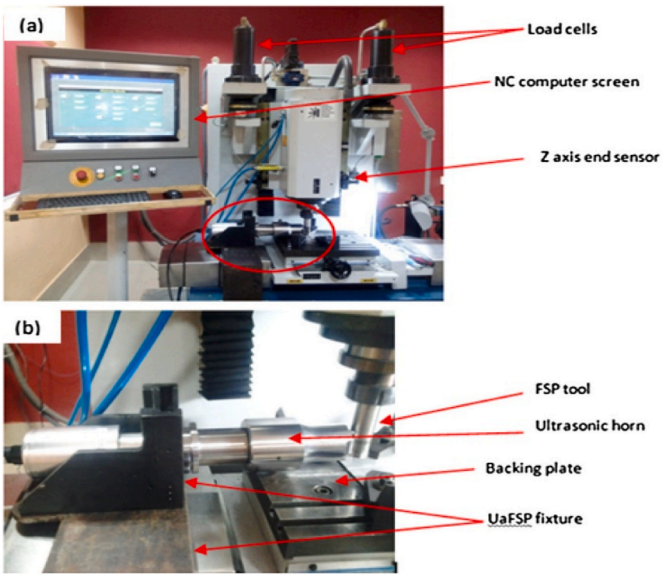

Fig. 7. Ultrasonic assisted FSP [62].

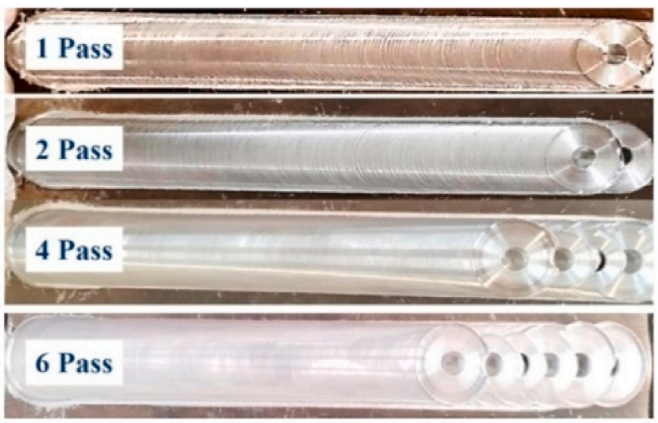

Fig. 8. Multi-pass FSPed samples with different numbers of passes [65].

plasticity behavior of FSPed Mg alloys and Mg composites, as documented and elucidated within the corpus of published literature. Initial literature survey was conducted with search keywords "friction stir processing", "Mg alloys", "Mg composites" and further filtered with "FSP of Mg alloys". Fig. 12 depicts the articles published within demographic area. It is drawn from the search that India, Iran, and China have most publications in the arena of FSP of Mg alloys. As China and India are the prominent suppliers of Mg alloys, more research on welding technologies have been conducted. Other countries, including Malaysia, Saudi Arabia, Canada, Nigeria, South Africa, Turkey, the UAE, Germany, Indonesia, and Australia, have also made intermittent but notable contributions to the research landscape.

3.1. Mechanical and microstructural improvements in FSPed Mg alloys

The requisite heat input for successful FSP is contingent upon the interplay of the substrate material's melting point and thermal conductivity. A lower material melting point corresponds to a reduced heat input requirement for FSP implementation [70]. Thermal conductivity, an inherent material property, governs the heat flow rate across a given area. Notably, Mg alloys, characterized by the lowest melting point among alkaline earth metals, exhibit distinct attributes in this regard. Specifically, their melting point (923 K) and thermal conductivity (156 W/mK) stand below those of Al and Cu alloys. This disparity translates into a diminished heat input necessity for FSP in Mg alloys, consequently reducing associated surface modification costs. For a visual representation of the thermal conductivity and ultimate strength profiles of Mg alloys and composites, refer to Fig. 13.

The interaction of thermal effects and severe plastic deformation within metallic substrates yields pronounced advancements in the microstructure of Mg alloys. Notably, a recrystallized configuration has been substantiated within the stir zone, alternatively termed the dynamically recrystallized zone (DXZ). A compendium of ongoing research endeavors centered on FSP-treated Mg alloys is catalogued in Table 2. This segment is dedicated to the presentation and comprehensive discussion of observed enhancements in microstructure and mechanical properties following FSP.

However, while FSP has emerged as an effective avenue for instigating fine-grain development across diverse Mg alloys encompassing the AZXX, AMXX, and ZKXX series, a particularly promising avenue for refining the texture of Mg alloys resides in the incorporation of rare-earth (RE) metals such as Ce, Gd, Y, Nd, and others [90,91]. Noteworthy scholarly efforts have recently explored the intricate texture mechanisms inherent in RE-Mg alloys [92,93]. The judicious inclusion of minute quantities of RE elements alleviates impurities and refines the microstructural attributes of Mg alloys [94]. Furthermore, certain RE elements, such as Y and Ce, exhibit the potential to augment flame retardancy and elevate the ignition temperature of Mg alloys [54,95]. The average grain size documented during FSP across distinct Mg-RE compositions is elucidated in Table 3.

Research by Yousefpour et al. [112] demonstrated a significant reduction in average grain size, from 61.6 μm in the as-cast sample to less than 10 μm in the FSPed AZ91 alloy, attributable to dynamic recrystallization (DRX). Utilizing FSP, Zhang et al. [113] also refined the microstructure of the AZ91 alloy, where DRX and fragmentation of the plate-like beta phase led to the formation of fine equiaxed grains around 3 μm in size within the α-Mg grains. Similar outcomes were observed in FSP treatments of cast AZ61 [114] and ZKX50 [115] alloys, resulting in considerable structure refinement. In another study, Wang et al. [116] conducted FSP on cast Mg–6Zn–1Y0.5Zr alloy, dissolving the coarse

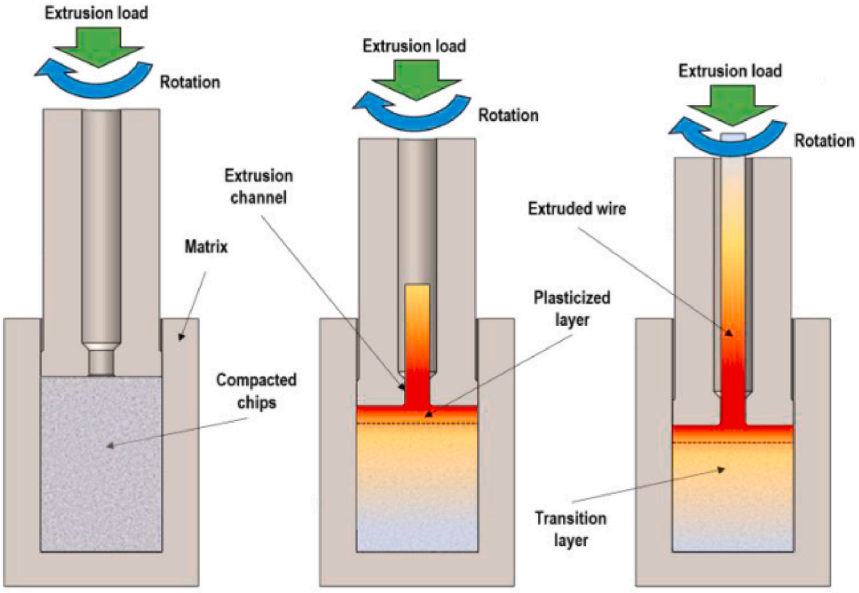

Fig. 9. Schematic diagram of Friction stir extrusion process [66].

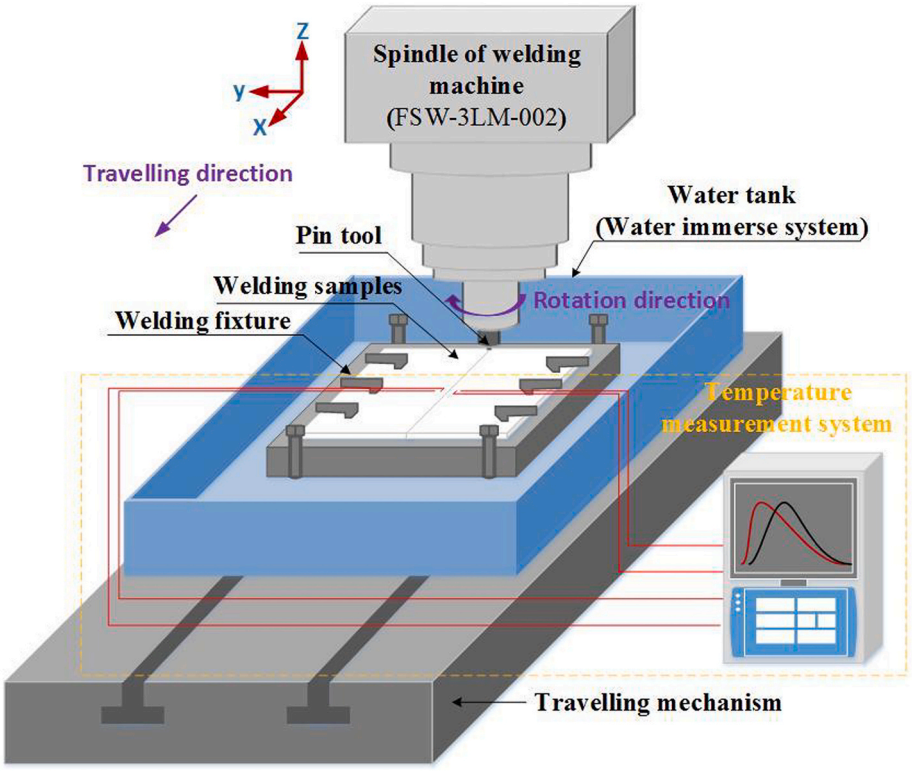

Fig. 10. Schematic representation of Submerged FSP [68].

eutectic I-phase network and refining grains, thus enhancing tensile characteristics. Jin et al. [117] investigated the influence of FSP on the microstructure and mechanical properties of as-cast Mg–Al-RE alloy, reporting improved mechanical performance post-FSP. Furthermore, Luo et al. [114] noted significant grain size refinement in the as-cast AZ61 plate due to DRX induced by FSP, with potential further refinement in subsequent treatments and detection of heterogeneous microstructures in the plate's periodic transition zones.

Transmission electron microscopy (TEM) observations have revealed that during FSP, a substructure of dislocations can be generated [6,27,28]. In a study focusing on an AZ31 alloy processed via friction stir, Fig. 14 presents TEM images of the SZ [118]. Fig. 14a depicts conditions with a rotation speed of 1000 rpm. Notably, a significant proportion of sub-grains is observed within the SZ, with a low density of dislocations confined inside the grains. Conversely, Fig. 14b corresponds to conditions with a rotation speed of 5000 rpm. Here, the fraction of sub-grains appears reduced, yet there is a notable increase in dislocation density both within the grains and along the grain boundaries. Furthermore, it is

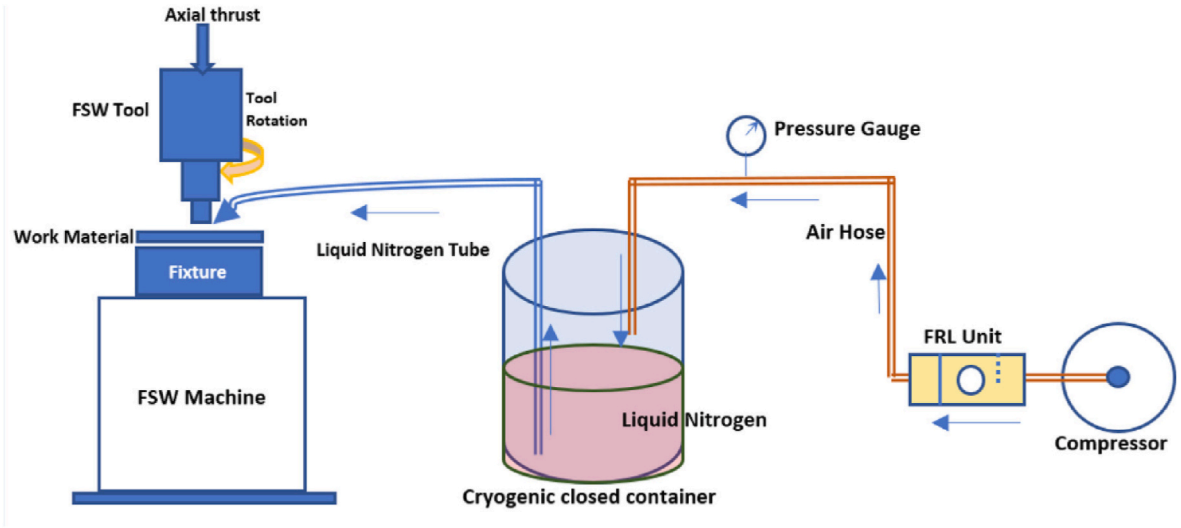

Fig. 11. Schematic arrangements of Cryogenic friction stir welding process [69].

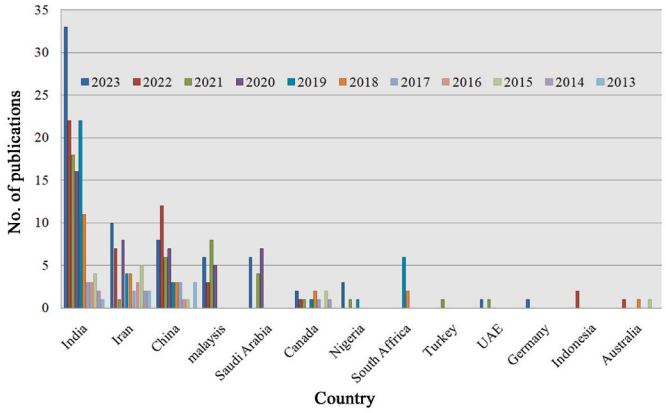

Fig. 12. Research articles published on FSP of Mg alloys and composites.

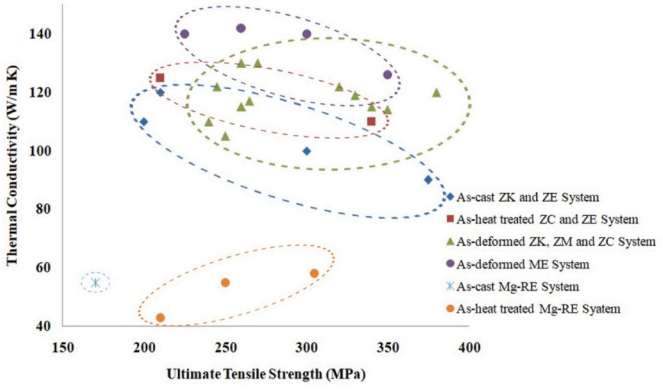

Fig. 13. Thermal conductivity and ultimate strength of some Mg alloys.

evident that the grain size under these conditions (Fig. 14b) is larger compared to the previous setting (Fig. 14a) [118]. These findings shed light on the intricate microstructural changes occurring during FSP processes and their correlation with processing parameters.

FSP induces significant alterations in the distribution and density of dislocations, as well as in the characteristics and distribution of phases and precipitations, marking a noteworthy evolution in material structure. Notably, the microstructural changes brought about by FSP can be observed in Fig. 15, which depicts TEM images and selected area electron diffraction (SAED) patterns of the SZ in the LZ91 alloy [119]. Fig. 15 showcases the SZ of the friction stir processed LZ91 alloy, revealing its composition of two distinct phases: α-Mg and β-Li. The interface between these phases, as well as the SAED patterns corresponding to zones A and B, are elucidated in the figure. Upon close inspection, it becomes evident that a minority of dislocations are situated near the boundary of the α-Mg phase, as depicted in Fig. 15a. Furthermore, the alternating black and white zones observed in Figs. 15b and c correspond to the α-Mg phase with a hexagonal close-packed (HCP) structure and the β-Li phase with a body-centered cubic (BCC) structure, respectively. The density of dislocations within the α-Mg phase appears notably higher compared to the β-Li phase, indicating a preference for plastic deformation within the latter during the FSP process [119]. This observation underscores the intricate interplay between microstructural features and mechanical behavior during FSP-induced transformations.

As we discussed earlier, FSP induces extensive alterations in the microstructure, substructure, and texture of materials. It was noted that FSP has the capability to convert the material surface into a composite, suggesting significant variations in the mechanical properties of friction stir processed materials. When alloys such as Mg alloys undergo FSP, several strengthening mechanisms come into play [120–122].

1. Grain Refinement Strengthening, also known as grain boundary or Hall–Petch strengthening, is observed. This process results in the formation of a fine-grained or ultra-fine-grained structure in the SZ [123]. Consequently, the Hall–Petch coefficient, which governs boundary pinning, significantly increases, leading to enhanced strength.
2. Orowan Strengthening is activated when secondary particles are dispersed within the microstructure through FSP. These particles, whether precipitates formed prior to FSW/FSP or induced during composite fabrication, trigger dislocation-particle interactions, known as the Orowan mechanism [124]. Notably, these precipitates or phases can exist in fine or ultrafine states, intensifying dislocation-particle reactions and thereby strengthening grain boundaries.
3. Solid Solution Strengthening occurs as precipitates and secondary phases potentially dissolve within the matrix phase during FSP. Additionally, homogenization effects associated with these processes contribute to the concentration of alloying elements within the matrix phase [125]. This increase in alloying element concentration further enhances the material's strength.

Table 2
Details of previous research on FSPed Mg alloys.

Researcher(s)	Material used	Observations
Del Valle et al. (2015) [71]	AZ31 Mg alloy	Authors controlled temperature at SZ and produced a grain size close to 0.5 μm. Super-plastic behaviour was observed at high temperature.
Zang et al. (2017) [72]	AZ31 Mg alloy	Authors obtained grain size of 10.4 μm from 1 pass, 10.4 μm in 2 passes, and 13.6 μm in three passes of FSP.
Raja et al. (2018) [73]	AZ91 Mg alloy	Authors used 720 rpm and 150 mm/min and reported that alpha phase of Mg dendrites in 100 μm was reduced to 2 μm by FSP.
MD and Panigrahi et al. (2018) [74]	QE22 Mg alloy	The interest of the authors was to investigate the high-temperature tensile deformation behavior of FSPed ultrafine-grained QE22 alloy at strain rate of 5×10^{-4} to 1×10^{-2} and temperature of 300 to 450 °C. They reported that it has shown high strain superplasticity at 450 °C with the highest elongation of 1630% at 1×10^{-2} s^{-1}. This result has been considered as a dual mode super plasticity demonstrated at high temperature and low strain rate.
Shang et al. (2019) [75]	AZ31 Mg alloy	Authors introduced profuse extension twins to the SZ of FSPed AZ31 alloy and reported that yield strength was increased from 96 to 122 MPa. Authors applied FSP after FSW was done on the material and hence it was a two-layered structure in SZ. This approach would work well for curved surfaces and hollow extruded 3D objects.
Zhang et al. (2019) [76]	AZ31 Mg alloy	Authors conducted FSP and surface mechanical attrition treatment (SMAT) on twin-roll cast plates. It was 6 mm thickness to improve the mechanical properties. They reported that FSP increased elongation higher than 40% and micro-hardness from ~60HV (base material) to more than 80 HV for FSPed surface. Also reported that yield strength was increased from ~52 to 70 Mpa after SMAT (34.6% increment).
Vasua et al. (2019) [77]	ZE41 Mg alloy	Authors reported that friction stir processing has reduced the grain size from 100 μm to 5 μm. Supersaturated grains were observed after FSP.
Peng et al. (2019) [78]	AZ31 Mg alloy	Authors investigated the microhardness at different depth of SZ of the processed Mg alloy and reported that top layer shows highest hardness as it had maximum dislocations.
Jin et al. (2019) [79]	AE42 Mg alloy	Authors reported the decrease of grain size from 81 μm to 7.4 μm. It is also reported that new Al_2RE phase appear after aging treatment as $Mg_{17}Al_{12}$ and $Al_{11}RE_3$ phases disappear after FSP.
Luo et al. (2019) [80]	AZ61 Mg alloy	Author's tensile tested AZ61 Mg alloy at strain rate of 1×10^{-2} to 3×10^{-5} and temperature of 473 to 673 K. Authors obtained grain size of 7.8 ± 6.4 μm after multi-pass FSP and reported the highest elongation of 211% at 623 K and 3.3×10^{-4} s^{-1}. It was caused by lower intensity of texture at that direction.
Seifiyan et al. (2019) [81]	AZ31B Mg alloy	Authors prepared samples by single-pass FSP and investigated their corrosion resistance using 35% NaCl. The best grain size from single-pass FSP was 15.9 ± 5.6 μm and the best from multi-pass FSP was10.2 ± 2.4 μm. Authors reported that exposure of chloride ions in a non-oxidizing Mg leads to pitting and corrosion is influenced by micro-constituents.
Fashami et al. (2020) [82]	AZ91 Mg alloy	Authors investigated the optimum FSP parameters for a defect-free sample. It was reported that 1200 rpm and 60 mm/min are optimum, where 23% increase in micro hardness, a 29% increase in tensile strength, and a 33% increase in creep strength at room temperature were observed. Subsequently investigation at 210 °C reported the tensile strength and creep strength increase by 31 and 47 %, respectively. Besides, high-speed processing (low heat generation) could lead to tunnel and groove defects, while low-speed processing (high heat generation) could result flash defects.
Sing et al. (2020) [83]	AZ91 Mg alloy	Authors reported that square pin profile is better than round pin profile as it uniformly distributes β-$Mg_{17}Al_{12}$ phase particles during corrosion resistance of AZ91 alloy.
Liu et al. (2020) [84]	AZ31 Mg alloy	Authors reported that four pass FSP has improved the corrosion resistance, but not tensile properties. It was reported that corrosion potential and corrosion current was increased from −1.56 to −1.19 V, and from 1.55×10^{-4} to 5.47×10^{-5} respectively.
Babu et al. (2020) [85]	ZE41 Mg alloy	The interest of authors was to investigate FSPed ZE41 Mg alloy for orthopedic implants. Weight lost due to deposition of more Ca/P mineral phase and reduced grain size from 107 ± 6.7 μm to 3.5 ± 1.5 μm was reported.
Patel et al. (2020) [86]	AZ31B Mg alloy	Authors reported that no external cooling is required when Cu backing plate was used in FSP. Hardness increase by 80% and tensile strength by 24% was observed.
Luo et al. (2020) [87]	AZ61 Mg alloy	Authors reported that appearance of β-$Mg_{17}Al_{12}$ phase in grain boundaries reduce the mechanical properties. FSP samples get higher because of dissolution of the large β-$Mg_{17}Al_{12}$ phase.
Kumar et al. (2021) [88]	Mg alloy	Authors reported that lower wear rate was found on friction stir processed sample at 600 rpm, where they evidenced grain size of 25 μm and hardness of 81 HV.
Wu et al. (2023) [89]	WE43 Mg alloy	Authors reported FSP effectively reduces the average grain size in WE43 alloy, enhancing its microstructure. It was 15.3% increase in hardness and 5% decrease in corrosion compared to the base material.

In general, it is important to note that the strengthening mechanisms discussed above not only impact yield strength but also affect tensile strength, ductility, and fracture energy. Research has shown that increasing tool rotation and decreasing welding speed enhances joint strength [126]. Additionally, studies confirm that among tool materials such as stainless steel, high-speed steel, armor steel, mild steel, and high carbon steel, superior tensile properties are observed in tools made of high carbon steel (specifically, threaded pins with a shoulder diameter of 18 mm) [127].

3.2. Corrosion and wear behaviour of FSP

Mg alloys are pivotal in the production of a diverse range of components; encompassing pressure die castings, body structures, and power train elements such as gearbox and engine components-cylinder bore and crankcase, where the interplay of relative sliding motion precipitates material loss attributed to friction and wear. Given the paramount significance of corrosion and wear resistance requirements, this discourse examines the studies and inquiries on the corrosion and wear resistance characteristics of FSPed Mg alloys.

Barathi et al. [128] embarked on a study delving into the effect of ageing duration and temperature on the corrosion resistance of FSPed AZ31 alloy. Their findings highlighted that heat-treated FSP Mg alloy

Table 3
Summary of Grain Size in FSP on Mg-RE alloys.

Rare Earth (RE) Mg alloy	FSP parameters			Grain size (μm)	References
	Rotational speed (rpm)	Travel speed (mm/min)	Shoulder diameter		
Mg–Mn–Ce	400	50	16	9.0	[96]
Mg-Gd-Y-Zr	800	100	5	6.1	[97]
Mg-Gd-Y-Zr	800	25, 50, and 100	20	5.6	[98]
Mg–Zn–Y–Zr	800	100	20	5.2	[99]
ZK60-Y	800	25, 50, and 100	20	4.7	[100]
Mg–Zn–Y–Zr	1500	100	20	4.5	[101]
Mg-2Nd-0.3Zn-1.0Zr	800	200	22	3.8	[18]
EV31A	400	102	25.4	3.4	[102]
GW103	800	50	20	3.0	[103]
Mg-Gd-Y-Zn-Zr	1500,2000, 2500,3000	25	20	2.8	[104]
Mg-1.2Zn-1.7Y-0.53Al-0.27Mn	500	101.6	11.5	2.8	[105]
WE43	275,300, 600	100	24	2.2	[106]
WE43	630	63	16	2.1	[107]
Mg-5.9Y-2.6Zn	450	50	20	2.0	[108]
Mg–Zn–Y–Zr	800	200	16	1.65	[109]
Mg–2Y-1.5Zn	1200	100	18	1.0	[110]
Mg-4.37 wt% Y-2.9 wt% RE-0.3 wt % Zr.	800 and 1250	63	16	1.98	[111]

subjected to FSP at 1200 rpm and 60 mm/min displayed remarkable improvement in corrosion resistance. Subsequently, Qin et al. [129] researched FSPed ZK60 Mg alloy supplemented with nano hydroxyapatite (HAp). Their investigation unveiled that the effects of reduced surface energy and grain refinement collectively bolstered corrosion resistance. Nano HAp disrupts the continuity of Mg grains, forming a protective layer over the FSPed sample.

Addressing a distinct corrosion phenomenon, stress corrosion cracking (SCC), characterised by crack propagation in corrosive environments such as chloride or H2S settings, emerged as a focal point of Huang et al. [130] study. Their research on FSPed A80 Mg alloy encompassed fine-grained (2.7 μm) and coarse-grained (7.1 μm) samples, revealing analogous basal texture attributes in both cases. Notably, FSPed Mg alloy demonstrated heightened corrosion and SCC resistance within a 3.5 wt% NaCl solution. Further investigations have unveiled nuanced distinctions in corrosion rates between FSPed AZ31B alloy specimens featuring step shoulder tools and those with concave shoulder tools, as underscored in Table 4.

Liu et al. [131] investigated a uniform corroded morphology in morphology in FSPed AZ91Mg alloy. Similarly, the corrosion resistance of FSPed and heat treated AZ91C alloy was systematically assessed by Hassani et al. [132] through the utilization of potentiodynamic polarization and immersion testing methodologies. Notably, both FSP and heat-treated specimens exhibited commendable corrosion resistance within the context of AZ91C alloy.

Undertaking an insightful inquiry, Huang et al. [133] meticulously analyzed the corrosion resistance of FSPed AZ80 Mg alloy, further subjected to subsequent ageing heat treatment. Employing potential dynamic polarization and immersion techniques, their study discerned compelling attributes, including super grain refinement, swift β-phase dissolution, and a noteworthy deviation of the c-axis from the transverse direction and processing direction. These observations collectively contributed to augmented static corrosion resistance and SCC resistance.

Zhu et al. [134] examined the metallurgical mechanisms and performance evolution of Mg–Li alloys during thermo mechanical processes. They observed that the alloy, when subjected to FSP with the highest heat input, demonstrated a significantly reduced corrosion current density of 6.10 × 10−6 A/cm^2, representing only 25% of that observed in the base metal. This improvement in anti-corrosion properties can be attributed to the dispersion and uniform distribution of precipitated particles induced by FSP. These particles act to impede micro-galvanic corrosion and facilitate the formation of a compact surface film, resulting in minimal and uniform corrosion across the material. Liu et al. [135] offered a noteworthy perspective by highlighting the superior corrosion resistance of single-pass FSP compared to the multi-pass FSP of ZK60 alloy. It is reported that the FSP effectively refines ZK60 alloy grains and enhances surface properties. However, multiple FSP passes don't further reduce grain size in the SZ and may increase grain size in the alloy. Additionally, additional FSP passes negatively affect the alloy's corrosion resistance and have limited positive impact on wear resistance in ZK60 plates.

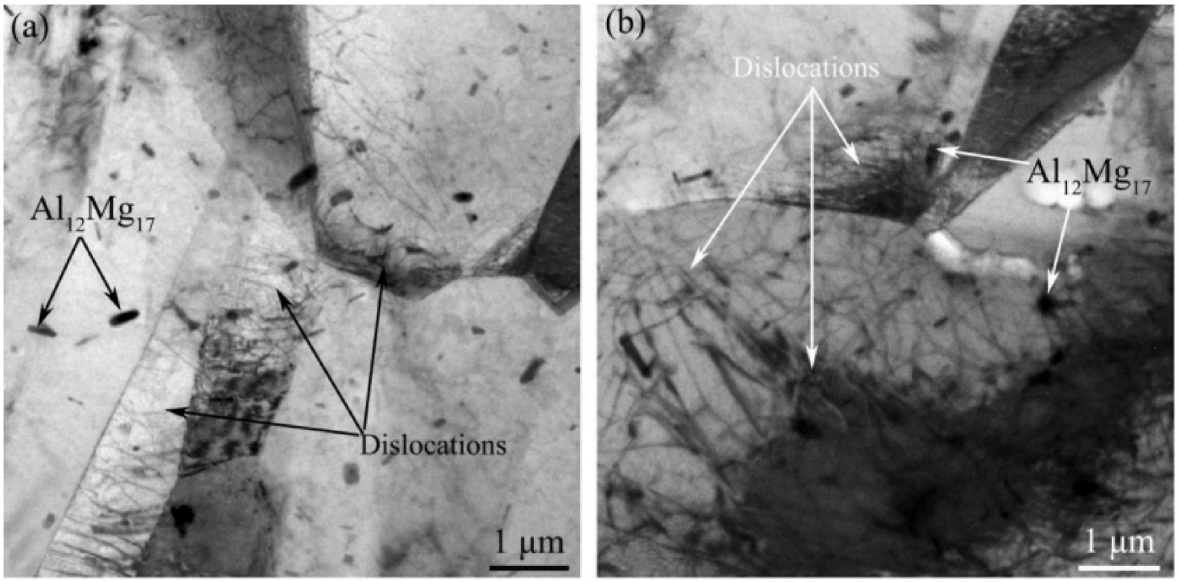

Fig. 14. TEM images of dislocations distribution at SZ of the friction stir processed AZ31 alloy: (a) rotation speed of 1000 rpm and (b) rotation speed of 5000 rpm [118].

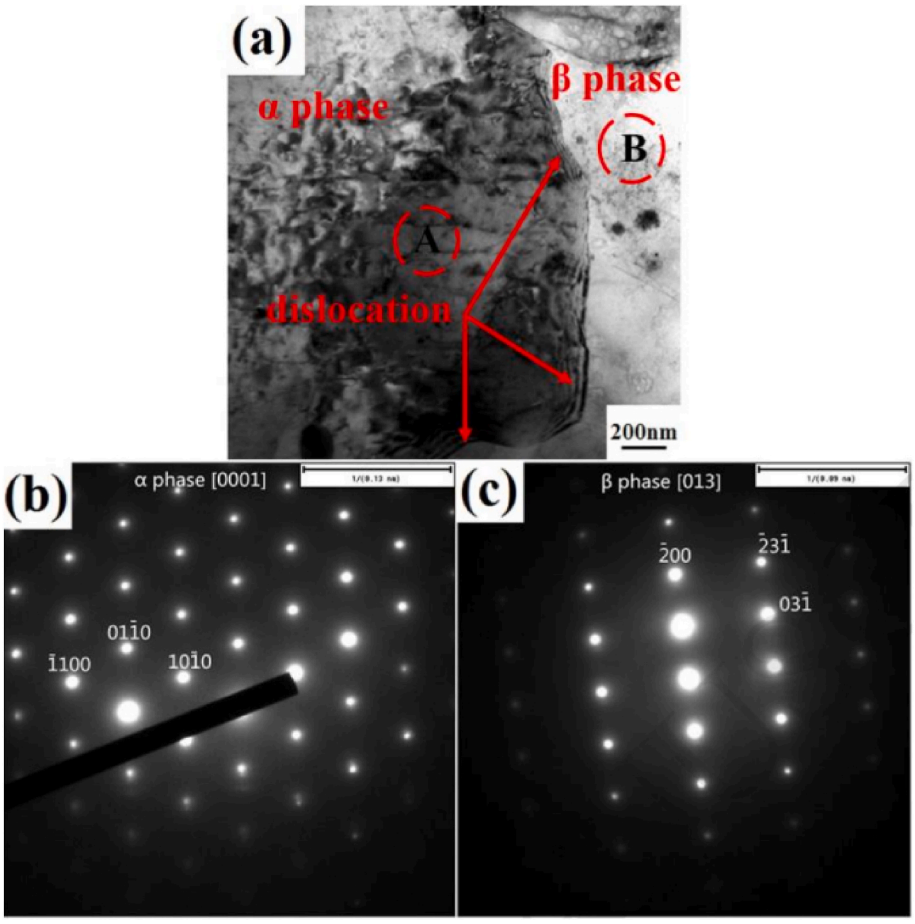

Fig. 15. TEM image and SAED patterns at SZ of the friction stir processed LZ91 alloy: (a) bright field image, (b) SAED pattern of A zone, and (c) SAED pattern of B zone [119].

Table 4
Corrosion rate of FSPed AZ31B alloy.

Tool profile	Speed (rpm)	feed (mm/min)	Corrosion rate (mm/yr)
Concave shoulder	500	20	0.0313938
	710	20	0.0153703
	1000	20	11.332273
Step shoulder	500	20	92.538
	710	20	112.73
	1000	20	84.702

Liu et al. [136] reported the corrosion resistance of cast Mg–9Al-xRE alloys upon immersion in a 3.5 wt% sodium chloride solution and exhibited notable deficiencies. This was attributed to the presence of coarse precipitated strips of Al-RE in the samples. Following FSP of Mg–9Al-xRE alloys, a distinct enhancement in corrosion resistance was observed, particularly evidenced in Fig. 16, where the alloy containing 6 wt% RE reinforcement displayed noteworthy corrosion resistance.

Arora et al. [137] conducted an investigation into the wear rate of FSP-treated AE42 alloy under varying loads (5–20 N) and velocities (0.33–3 m/s). Their findings underscored a maximum wear rate at the lowest velocity and highest load, revealing diverse wear mechanisms in the FSPed AE42 alloy, as depicted in Fig. 17. Rathinasuriyan and Sankar [138] elucidated that cryogenic FSPed AZ31B alloy exhibited a 20% reduction in wear rate compared to its cast Mg alloy counterpart. Adopting a spiral tool path strategy for FSP on AZ91D alloy, Kumar et al. [139] illustrated how tool rotation influenced the occurrence of tunnel defects, with tool shoulder overlaps aiding in defect mitigation. They identified the wear rate under optimized conditions and observed higher wear on the non-FSPed AZ91D sample compared to FSPed samples.

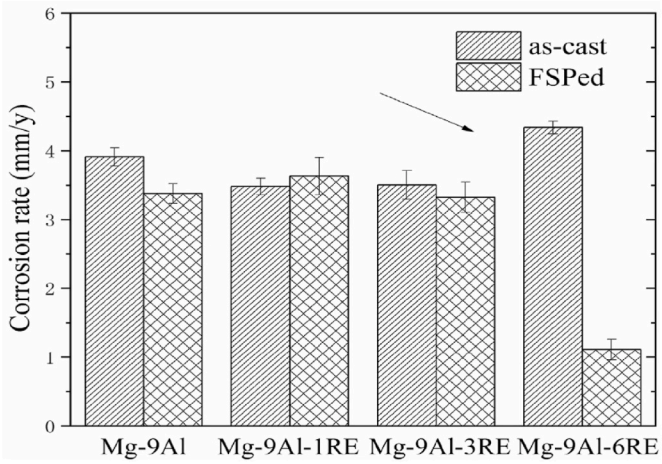

Fig. 16. Corrosion rate of Mg–9Al-xRE alloys [136].

3.3. Formability studies conducted on FSPed Mg alloy

Mg alloys exhibit limited formability at ambient temperatures due to their inherent hcp crystalline structure. However, the implementation of FSP imparts notable enhancements in ductility and formability. Noteworthy investigations have been undertaken to discern the effects of FSP

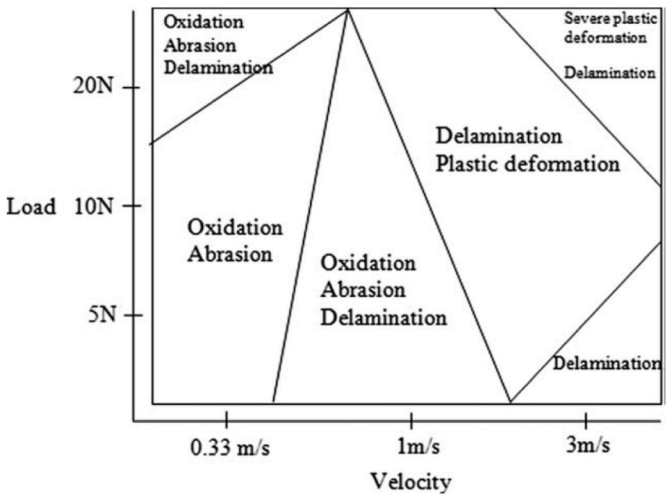

Fig. 17. Wear map for the FSPed AE42 alloy [137].

on these attributes.

Hutsch et al. [140] systematically evaluated formability behaviour in a study employing a multiline sample configuration, as depicted in Fig. 18. Their findings indicated a progressive enhancement in formability with increasing processing speed. Delving into superplasticity, Cavaliere and Marco [141] explored the superplastic performance of an FSPed AZ91 Mg alloy. The study attributed the exceptional ductility to attaining an ultrafine grain structure through the FSP process. Examining optimal parameters for enhanced formability and heightened mechanical properties, Venkateswarlu et al. [142] established that a shoulder diameter of 18 mm and an overlapping ratio of 1 yielded a homogenized and equiaxed surface conducive to formability. Their study encompassed critical parameters such as limiting dome height, strain hardening rate, and work hardening capacity. Fig. 19 graphically represents the outcomes, indicating that an overlapping ratio of 1 exhibits superior formability compared to alternative ratios.

Venkateswarlu et al. [143] explored the formability of AZ31B alloy after FSP. This investigation assessed crucial formability attributes, including the maximum limiting dome height and strain limits. These characteristics were analyzed using forming limit diagrams and statistical models, yielding insightful predictions.

In a parallel study, Wang et al. [144] delved into the superplastic deformation exhibited by FSPed AZ80 Mg alloy. The process engendered a distinctive transformation in texture alongside significant grain refinement within the AZ80 Mg alloy. This enhanced texture and refined grain structure conduced to a favorable environment for superplastic deformation, facilitated by the initiation of prismatic and pyramidal slips.

In corresponding work, Ramesh Babu et al. [145] undertook FSP on AZ31B alloy, explicitly focused on altering key process parameters such as traversing speed, axial force, and rotational speed in FSP of AZ31B alloy and observed noteworthy reductions in forming time, achieving an approximate 18.5-fold decrease compared to the base material. The goal was to attain a dome height of 31.5 mm under specific conditions of 350 °C and 0.4 MPa. The pertinent details, including forming temperature, strain rate, and the super-plasticity behaviour of FSPed Mg alloys, are systematically presented in Table 5.

3.4. Nano particles reinforced Mg metal matrix composite through FSP

FSP presents a versatile avenue for fabricating Mg metal matrix composites (MMC) by strategically incorporating nanoparticles within the surface region. This methodology imparts localized strengthening effects while fostering a homogenized microstructure. Diverse strategies have been employed to disperse reinforcing phases within the metal matrix, leading to the creation of MMCs via FSP (refer to Fig. 20). A prevalent approach involves embedding secondary particles into pre-machined grooves on plate surfaces before engaging in the FSP procedure [69].

The integration of nanoparticles, such as SiC [152,153], Al_2O_3 [154,155], TiC [156], Ti [157], and carbon nano tubes [158,159], into Mg alloys via FSP has demonstrated the capacity to enhance the mechanical properties of the Mg alloy matrix in localized regions. Introducing ceramic particle reinforcements or secondary phases plays a pivotal role in augmenting the occurrence of critical dynamic recrystallization during FSP [160,161]. Consequently, the stacking fault energy (SFE) emerges as a critical determinant governing the microstructural behaviour of MMCs, exerting a substantial influence over the ensuing material characteristics [162].

In this context, the integration of nanoparticles within the matrix triggers the particle-stimulated nucleation (PSN) recrystallization

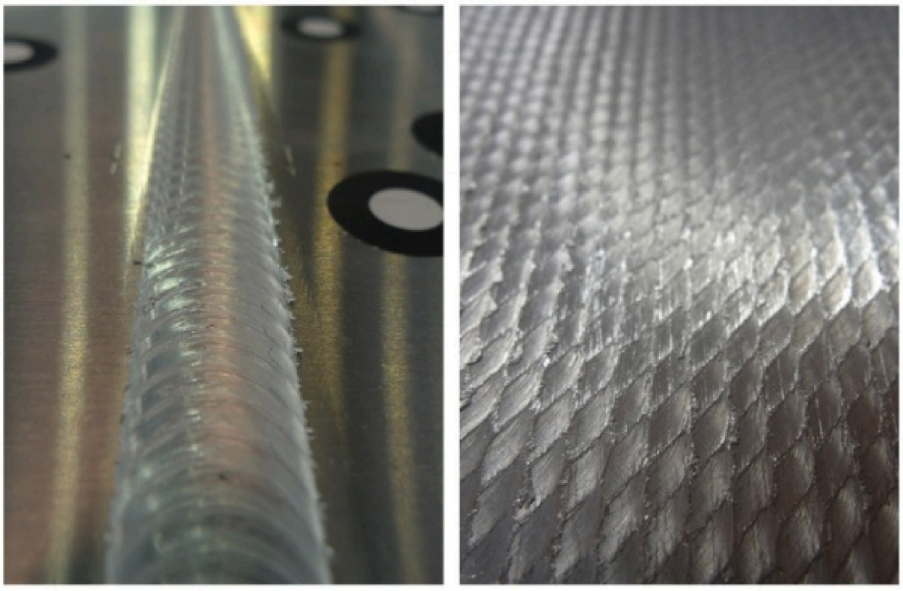

Fig. 18. Singe pass and multi-pass specimen [140].

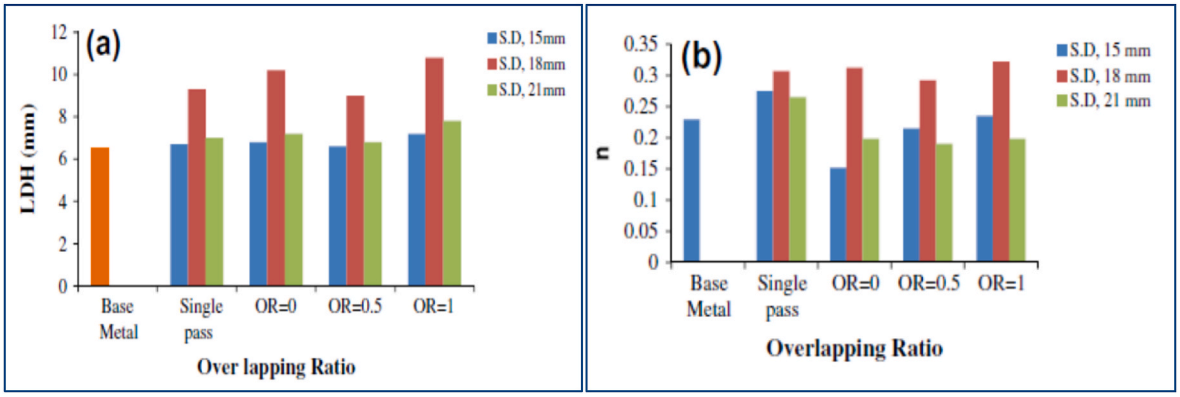

Fig. 19. Impact of overlapping ratio (a) LDH (b) strain hardening rate [142].

Table 5
Super-plasticity behaviour of FSPed Mg alloys.

Mg Alloys	Temperature (°C)	Strain rate (s^{-1})	Super-plasticity behaviour	References
AZ91	350	2×10^{-2}	High Strain Rate Super-plasticity (HSRS)	[113]
AZ91	300	5×10^{-4}	LTSP	[146]
AZ61	300	1×10^{-4}	–	[147]
AZ31	450	1×10^{-2}	HSRS	[148]
AZ80	300	1.4×10^{-4}	–	[149]
WE43	375	3×10^{-4}	–	[150]

mechanism. This phenomenon is instrumental in instigating pronounced Zener-pinning effects, ultimately culminating in developing ultrafine-grained microstructure. Despite its remarkable potential, it is noteworthy that FSP remains relatively underutilized as a method for surface treatment. This situation underscores the yet-to-be-explored avenues and untapped potential that FSP holds in enhancing material properties and optimising structural characteristics. The intrinsic capacity of FSP to harness the synergistic effects of nanoparticles and advanced processing techniques suggests a promising realm for further research and application across diverse industrial domains [163].

The enhancement in tensile strength observed in Mg MMCs can be attributed to the combined effects of finer grains and the pinning phenomenon induced by the incorporation of reinforced particles during the FSP [164,165]. A scanning electron microscope micrograph of the processed zone of a Mg alloy reinforced with TiC nanoparticles is presented in Fig. 21, showcasing various levels of nanoparticle volume addition. Notably, Fig. 21 (c and d) highlights the distinctive characteristics of a refined Mg-matrix with finely dispersed TiC nanoparticles, illustrating the potential for grain refinement through the reduction in mean size and increase in reinforcement particle volume fraction.

TEM image of 5 vol% TiC reinforced Mg composite is shown in Fig. 21a. It evidences the fine and continuous rings of TiC particles over the selected area diffraction pattern. This observation is further corroborated by the bright and dark field TEM micrographs, which also emphasize the fine grain size of the Mg matrix.

Consequently, a comprehensive summary of research endeavors

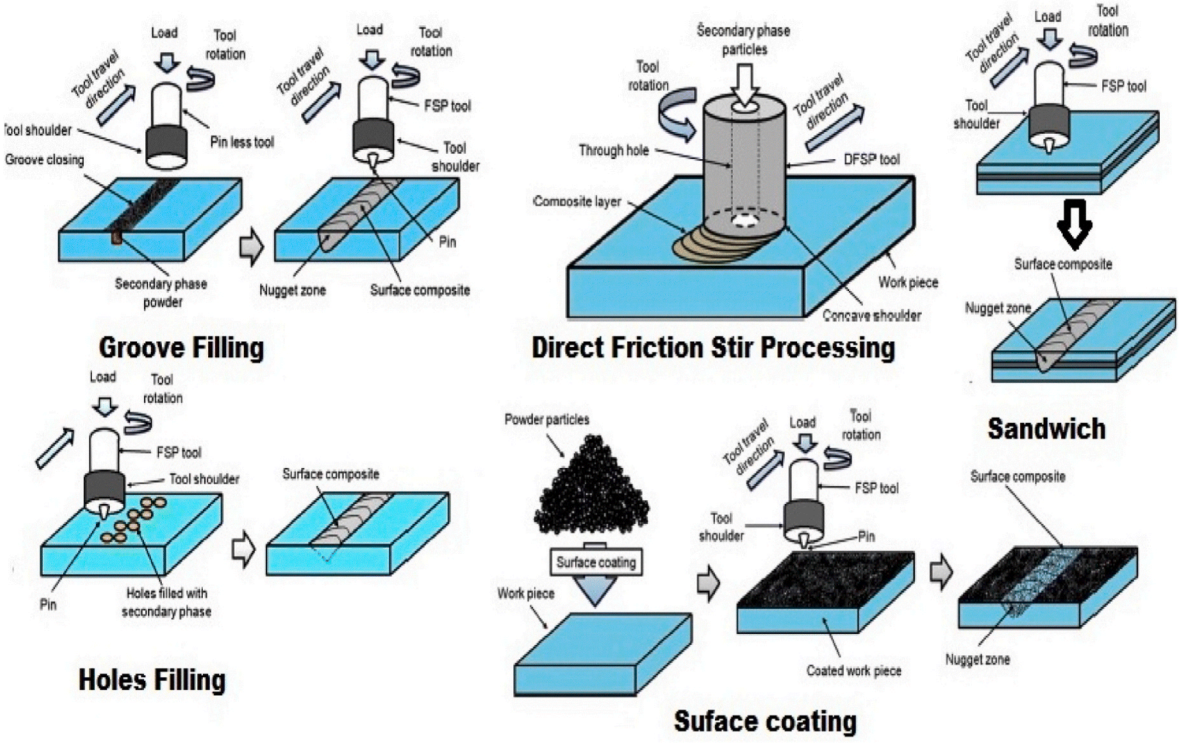

Fig. 20. Strategies of secondary phase incorporation [151].

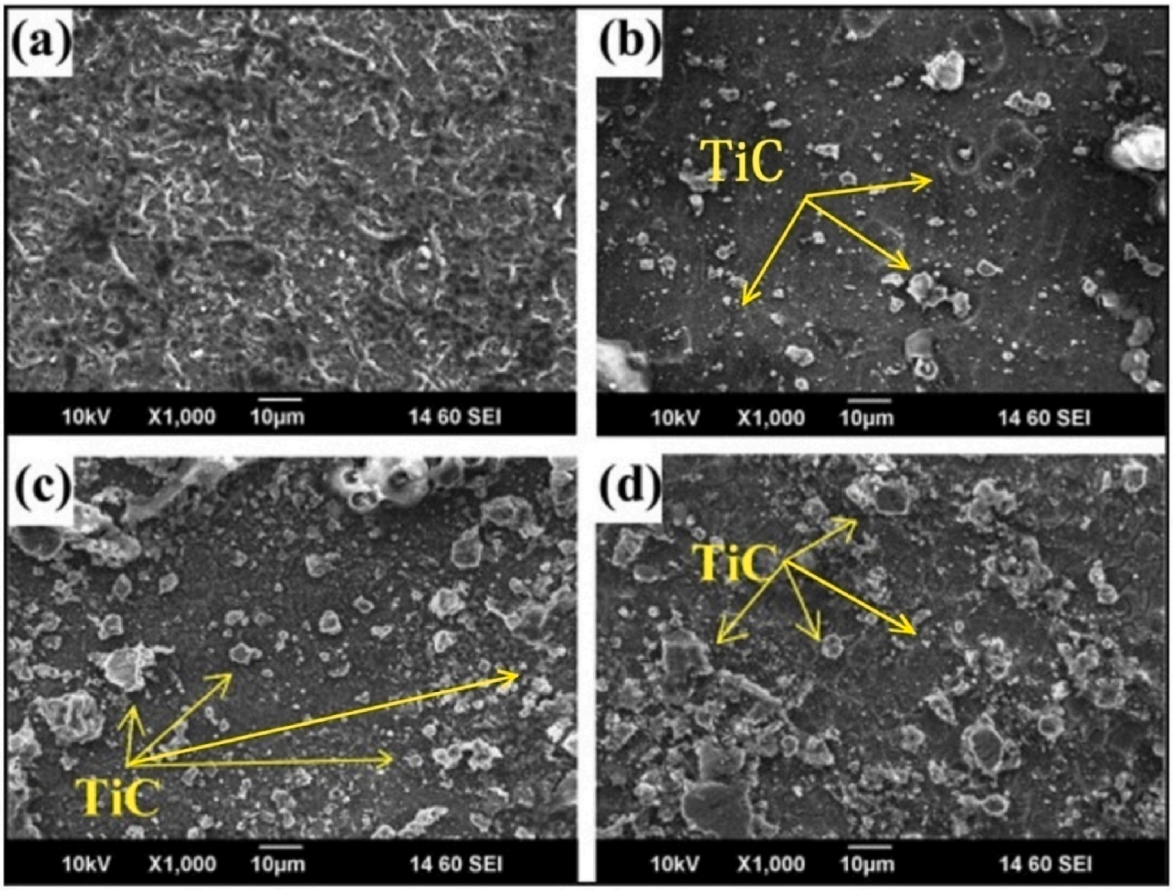

Fig. 21. SEM image of AZ31/TiC Composite (a) 0 vol% TiC (b) 6 vol% TiC (c) 12 vol% TiC (d) 18 vol% TiC [156].

involving FSP of Mg alloys reinforced with various particles is compiled in Table 6. The data presented in Table 6 collectively underscore the profound impact of FSP on mechanical and tribological properties in particles-reinforced Mg alloys.

Table 6
Nanoparticles reinforced FSPed Mg alloy.

Base Material	Reinforcing Particles	Conclusion/Remarks	Reference
AZ91	SiC	Increase in tensile strength and elongation was reported as SiC nanoparticles had a significant impact on the SZ's grain refinement	[166]
AZ91	Al_2O_3	Increase in wear characteristics and hardness was reported as homogeneous distribution of Al_2O_3 particles was achieved	[167]
AZ91C	SiO_2	Improved mechanical strength was reported after multi pass FSP with SiO_2 reinforcement	[168]
WE43	Hardystonite	Reduced corrosion rate was reported as Hardystonite significantly reduced localized corrosion of the WE43 alloy after FSP	[169]
AZ91	SiC	Reported that refined surface composite layer of AZ91/SiC can be achieved by an increase in tool rotating speed	[170]
ZK60	nano-hydroxyapatite (nHA)	Reported that addition of second phase particles effect the high corrosion resistance	[171]
AZ31	TiC	Reported that increase in mechanical properties can be achieved by clustering TiC in SZ	[156]

4. Potential areas to be explored in coming years

Though we understand that substantial research pinning to FSP of Mg alloy has been conducted in the past, there are some avenues, still many research findings have not been explored or identified. This section explores them and opens up some of the key areas that the research must be taken up in the future.

4.1. Influence of FSP underwater medium

A spectrum of conditions encompassing water, cold water, hot water, and cryogenic environments have been explored in FSP, each yielding distinct enhancements in microstructure and mechanical properties. This segment is dedicated to elucidating the outcomes of research efforts on underwater FSP, delving into its discernible effects on pivotal mechanical parameters including tensile strength, yield strength, hardness, grain size, and elongation percentage.

Sankar et al. [172] conducted a comprehensive investigation wherein conventional FSP in air and submerged friction stir processing (SFSP) were evaluated regarding their impact on microhardness. This inquiry systematically explored varying rotational speeds ranging from 500 to 1000 rpm, coupled with different welding speeds spanning 50–350 mm/min. The findings contribute to an enriched understanding of the distinct effects elicited by the SFSP paradigm. Three distinct cylindrical (CL) pin profiles namely, scrolled stepped square (SSSQ), scrolled stepped (SSCL), and scrolled (SCL) pins were meticulously examined. The SSSQ tool configuration notably demonstrated heightened hardness within the stir zone relative to the alternative pin profiles,

as illustrated in Fig. 22. This phenomenon can be attributed to the pulsation effect, inducing a more pronounced plastic deformation within the processed material.

Asadi et al. [173] ventured into the realm of in-process water cooling effects on the mechanical and microstructural attributes of FSPed AZ91 Mg alloy. Their study revealed a concurrent elevation in hardness alongside a reduction in grain size within the water-cooled processed specimens. Similarly, an exploration by Ramaiyan and Kumar [174] centered on SFSP, explicitly focusing on hot-rolled AZ31B Mg alloy. The outcome showcased a superior microstructural refinement, which augmented tensile properties and microhardness within the processed material.

Further insights were provided by Alavi Nia et al. [175], who investigated the interplay of water cooling conditions, pin profiles, and traverse speed during FSP of AZ31 Mg alloy. The cooling action engendered a discernible reduction in grain size coupled with heightened hardness, strength, and ductility. Additionally, an optimal speed of 58 mm/min was identified, yielding the highest mechanical properties when contrasted with 28 and 40 mm/min. Darras and Kishta [176] extended their investigation to encompass water and air environments, conducting FSP on AZ31 Mg alloy. Their study scrutinized the effects of thermal fields, grain size, and tensile properties within these contexts. A comprehensive overview of tensile properties across unprocessed and SFSP scenarios encompassing air, hot water, and cold water environments is systematically presented in Fig. 23.

Luo et al. [177] investigated mechanical properties of SFSPed Mg

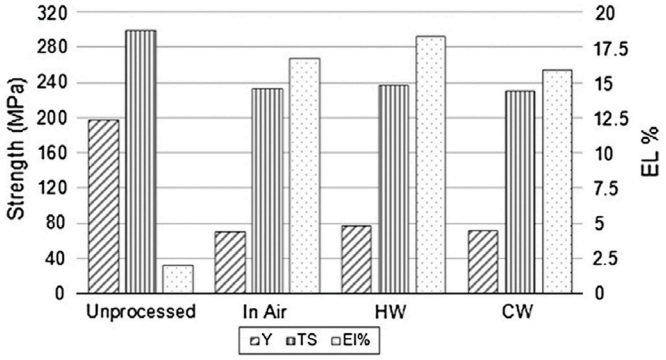

Fig. 23. Tensile behaviour of SFSPed AZ31 alloy [176].

samples with single-pass and double-pass. Table 7 summarizes tensile properties for BM, single-pass, and double-pass SFSP specimens.

The study conducted by Cao et al. [178] entailed a meticulous examination of macrographs of Mg–Nd–Y alloys subjected to both submerged and conventional FSP techniques. Remarkably, the width of the SZ was 6.59 and 6.73 mm for submerged FSP and ordinary FSP, respectively. Notably, the implementation of submerged FSP was found to induce an advanced cooling effect, resulting in improved outcomes. An investigation by Huang et al. [130] further delved into the structural and property alterations in underwater FSPed AZ80 Mg alloy. The

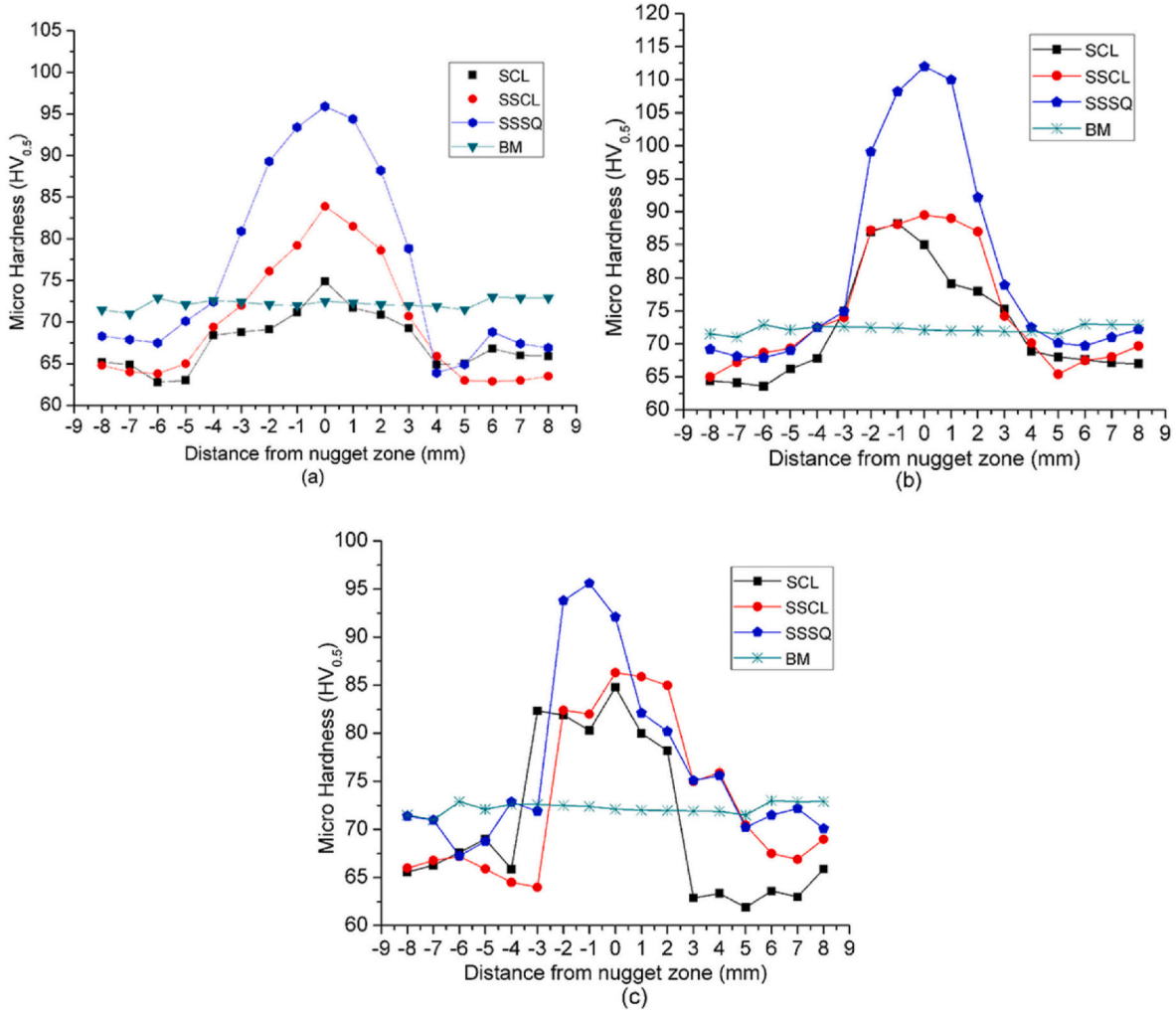

Fig. 22. Micro-hardness of SFSP with different pin profiles (a) 800 rpm (b) 1000 rpm (c) 1200 rpm [172].

Table 7
Mechanical properties in different conditions.

	Yield Strength (MPa)	Ultimate Tensile Strength (MPa)	% of elongation
Base material	74	115	9.21
Single pass FSP	108	289	28.13
Double pass FSP	100	286	37.21

processed zone resulting from air-based FSP was notably more minor than the water-based FSP samples. This disparity was attributed to the accelerated cooling rates characteristic of SFSP. Fig. 24 visually captures the macrostructural discrepancies between air and water specimens.

Moreover, the work undertaken by Chai et al. [179] involved the utilization of SFSP on AZ31 alloy, exploring fixed traverse settings while varying rotational speeds. The investigation additionally scrutinized the effect of rotational speeds on the resulting microstructures of the processed samples. The study unveiled notable insights regarding grain sizes, wherein the underwater FSP samples exhibited grain sizes of 2.8, 3.3, and 3.8 μm at 1100, 1300, and 1500 rpm, respectively. The observed trend indicated an increase in grain size with escalating rotational speeds. The authors concluded that SFSP demonstrates a distinct potential for producing fine-grained materials.

In a related exploration, Cao et al. [180] embarked on SFSP, focusing on Mg–Y-Nd alloy under controlled conditions of a constant speed of 600 rpm and a feed rate of 60 mm/min. The experimental setup encompassed a tool with a tilt angle of 2.5°, a threaded conical pin with a diameter of 4 mm, and a shoulder diameter of 15 mm. The results highlighted the efficacy of SFSP, with a grain size of 1.3 μm—a substantial improvement compared to the base alloy with a grain size of 54 μm. This significant grain size reduction was attributed to the accelerated cooling effect inherent in SFSP.

Further exploration by Chai et al. [181] encompassed both FSP and SFSP of AZ91 alloy revealed a pronounced disparity in the volume fraction of β-Mg17Al12 particles between normal FSP and SFSP specimens. This disparity was attributed to the heightened cooling rates characteristic of SFSP, thus contributing to the observed variation. Luo et al. [182] established a comprehensive correlation between the tensile properties and microstructural attributes of multi-pass SFSPed AZ61 Mg alloy. The analytical study unveiled a distinctive grain size of 3.7 μm for the multi-pass SFSP samples. Notably, the application of rapid water cooling effectively suppresses the re-precipitation of the β-Mg17Al12 phase. Consequently, a limited presence of precipitation particles was observed near grain boundaries, a phenomenon highlighted in Fig. 25.

The empirical implications of prior research findings concerning SFSP are elaborated below, encompassing the domains of temperature distribution, corrosion resistance, wear behaviour, and super plasticity

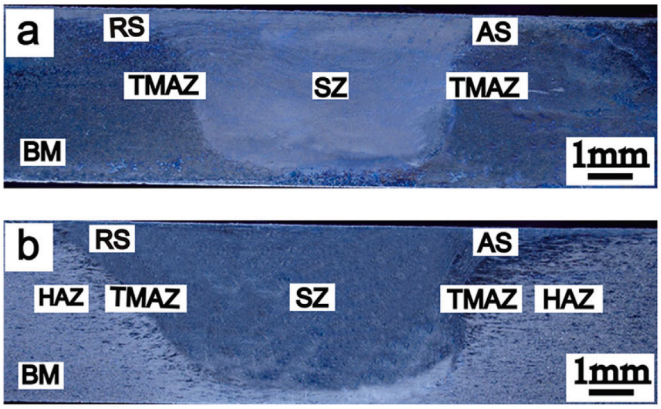

Fig. 24. Macroscopic image (a) FSP (b) SFSP [130].

tendencies across various Mg materials:

In a comprehensive investigation conducted by Chai et al. [183] revealed that SFSP approach exhibited a notably lower peak temperature and a significantly accelerated cooling rate when contrasted with conventional FSP. Similarly, Iwaszko and Kudła [184] delved into FSP of AZ91-D Mg alloy in air and underwater environments. The wear testing was particularly interesting, which facilitated a direct comparison of wear performance between FSP under air and water conditions. Notably, the FSP underwater medium specimen demonstrated enhanced wear resistance as opposed to the FSP specimen in an air-based environment. Exploring the effects of wear behaviour on water-cooled FSPed samples, scrutinized load and sliding velocities variations, utilizing Mg alloy AE42 as the focus material. Remarkably, the FSP specimens exhibited a substantial reduction in wear rate, a phenomenon attributed to microstructural alterations leading to improved microhardness and ductility within the processed samples.

Ramaiyan et al. [185] meticulously explored FSP within an underwater environment, employing the L_{27} orthogonal array approach for AZ31B alloy. The investigation encompassed tool pin profile, rotational speed, and processing speed. Remarkably, a notably low corrosion rate of 0.011748 mm/year was achieved under specific conditions: a processing speed of 1.0 mm/s, a rotational speed of 1000 rpm, and the stepped square pin profile utilization. Furthermore, Cao et al. [180] successfully demonstrated the exceptional super plasticity of SFSPed Mg–Y-Nd alloy. This achievement was underscored by an impressive elongation of 900 % observed at 758 K, coupled with a strain rate of $2 \times 10^{-2}\ s^{-1}$. The observed enhancement in elongation can be attributed to the synergistic effects of the fine-grained microstructure and superior thermal stability. The nuanced relationship between elongation and strain rate for the SFSPed samples is visually depicted in Fig. 26.

Cao et al. [186] in their other research examined the dynamic evolution of microstructure and superplastic behaviour within Mg–Y–Nd alloys. Their study demonstrated the successful achievement of fine-grained structures through SFSP conducted underwater. This refined microstructural configuration proved pivotal in attaining a remarkable maximum elongation of 967 %. Similarly, Datong et al. [187] investigated the tensile and super-plastic properties inherent to underwater FSP of Mg–9Al–1Zn alloy. Their comprehensive study yielded favorable results, including a notable strain rate response and an impressive elongation of 990 % in the FSPed material. The graphical representation of nominal stress reduction at strains exceeding 0.6 and the visual depiction of tensile specimens is illustrated in Fig. 27.

In summary, this section underscores the pronounced influence of the medium on the heat dissipation process. It is evident that water exhibits a superior heat capacity compared to air, resulting in a notable acceleration of the cooling rate during SFSP in contrast to the conventional FSP conducted in an air medium. This divergence is manifested by a reduction in the peak temperature observed during SFSP. The strategic manipulation of heat energy within the processed zone and the heightened cooling rate induced by the underwater environment are pivotal factors in mitigating grain growth within the processed zone. This meticulous control not only engenders a refined microstructure but also underscores the attainment of enhanced mechanical properties, thus reinforcing the interplay between controlled thermal dynamics and resultant microstructural enhancements.

4.2. Cryogenic-cooling friction stir processing (CFSP)

A review of FSP under cryogenic medium (LN_2) and relevant literature deals with LN_2 is provided below.

An empirical investigation focusing on torque, temperature, and grain size reduction in cryogenic condition was undertaken by Ammouri et al. [188]. An analysis of FSP under air-cooled specimens revealed a decrease in impact strength and tensile strength and an increase in elongation at cryogenic temperatures. A remarkably fine-grained microstructure of approximately 300 nm was achieved using FSP

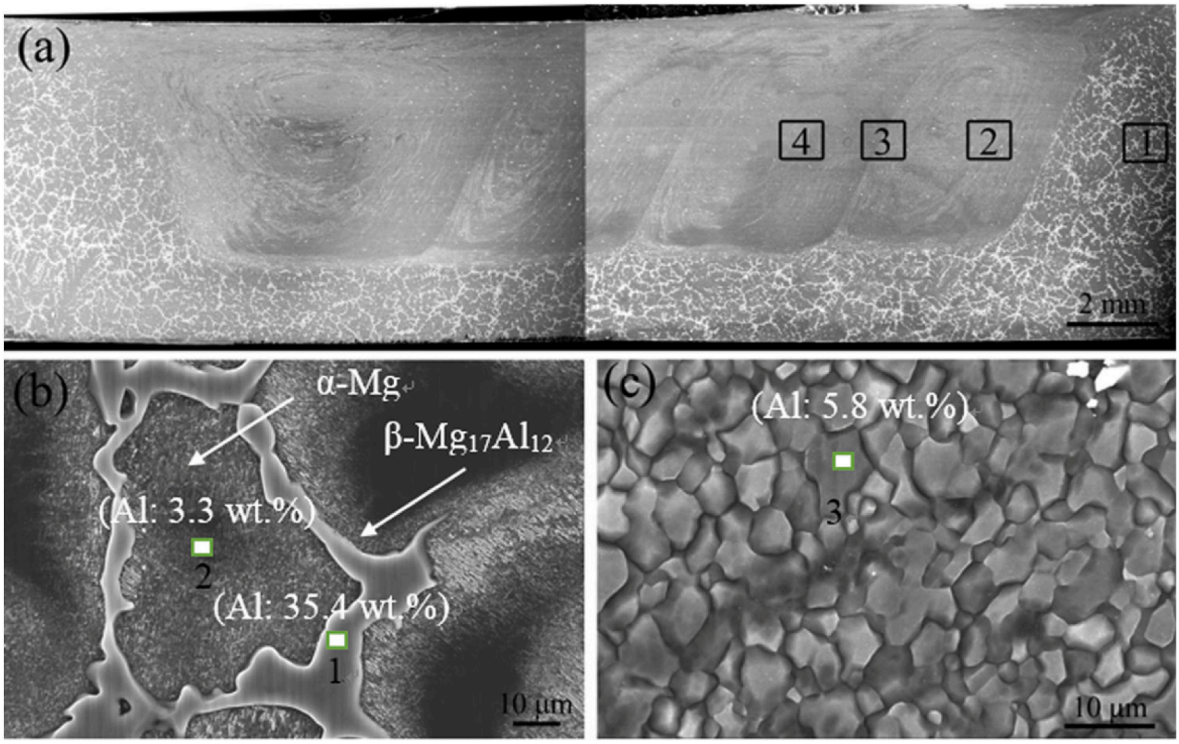

Fig. 25. a) Macroscopic morphology of cross section of SFSPed alloy, and the microstructure of b) BM and c) SFSPed samples [182].

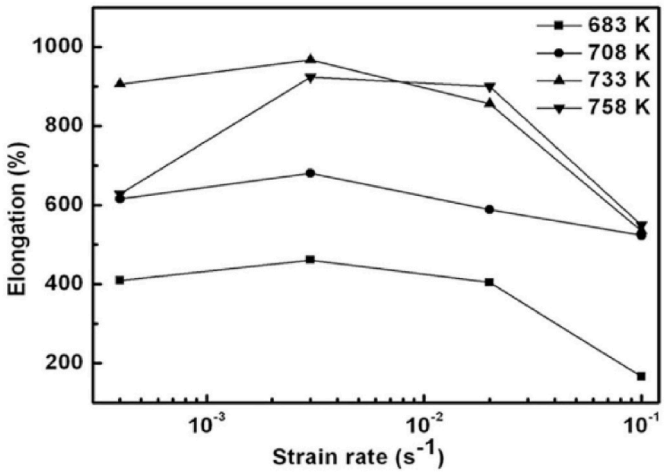

Fig. 26. Elongation with strain rate for the SFSP samples at different temperatures [180].

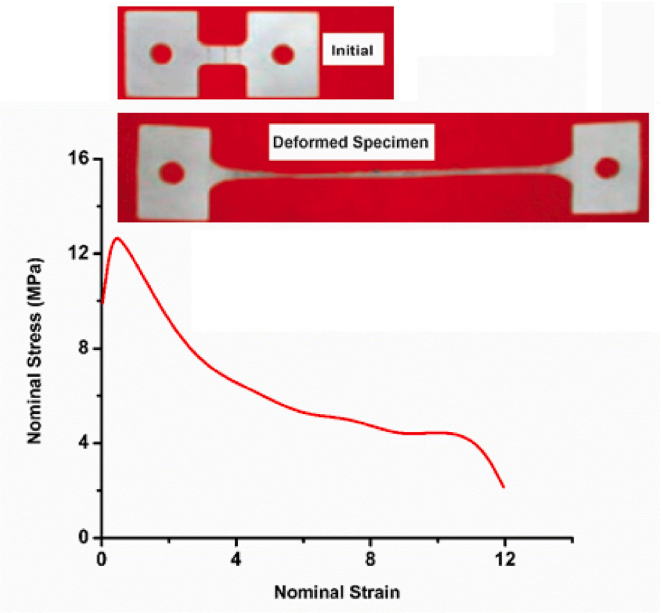

Fig. 27. Normal stress Vs Normal strain graph of super-plastic tensile behaviors of SFSP specimen [187].

within a liquid nitrogen medium [189]. The enhanced cooling effect contributed to developing a refined grain structure with a smoother interface, resulting in improved ductility and reduced cleavage fracture, thus enhancing overall material performance. Investigating the microstructural effects of FSP and SFSP on Mg alloy, another study utilized a constant speed of 800 rpm and a feed rate of 40 mm/min, employing a tool with a 15 mm diameter shoulder [190]. The SFSP samples exhibited superior strength and elongation than the standard FSP samples. The temperature, torque, and mechanical properties of cryogenically processed Mg alloy were explored by a study conducted by Rao and Naik [191] revealing a decrease in impact strength and tensile strength alongside an increase in elongation. Furthermore, FSP was conducted on AZ31B Mg alloy under varied cooling conditions [192]. The findings illustrated in Fig. 28 showcased the effects on elongation, tensile strength, and hardness across three different processing conditions. The cryogenic FSPed sample exhibited a slight reduction in tensile strength and hardness but an increase in elongation compared to the SFSPed sample.

In a notable study, Chang et al. [193] identified a significant challenge rooted in their prior experience with FSP, namely the critical issue of heat dissipation during the process. To mitigate this challenge, they ingeniously employed a thin copper mould as a heat sink and harnessed the cooling capabilities of liquid nitrogen. Their innovative approach

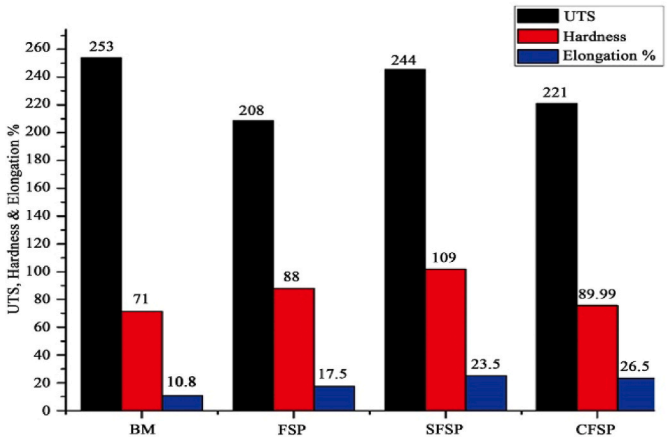

Fig. 28. Mechanical properties of FSP under various mediums [192].

yielded an ultrafine and uniformly grained microstructure. This achievement of ultrafine grains contributed to a notable improvement in the hardness of the processed sample. In a similar vein, Du and Wu [194] undertook FSP with the utilization of a rapid heat sink, aiming to achieve fine grain refinement in AZ61 alloy. Their efforts resulted in a microstructure characterized by grains as small as 300 nm. Moreover, strategically employed cryogenic cooling to enhance the grain size in FSPed AZ31B Mg alloy, further illustrating the ongoing exploration of cryogenic techniques in this field of research [195]. The finer and homogeneous microstructure was observed from cryogenically cooled specimens than the room-temperature samples. For instance, the grain size for the cryogenically cooled FSP was 6 μm when these authors applied multiple-pass FSP. The resulting grain sizes under different cooling conditions are summarized in Table 8 for reference.

In a comprehensive study by Mohammed [196] reported the effect of cryogenic cooling on the corrosion rate of FSPed AZ91 alloy. Authors reported that increase in microhardness after cryogenic cooling is caused by the enhancement in grain structure and the distribution of β-phase constituents. Similarly, Ammouri et al. [188] conducted a comprehensive assessment of the impact of liquid nitrogen on the FSP process applied to AZ31B alloy. The experimental campaign involved varying rotational and welding speeds while assessing pertinent parameters such as thrust force, torque, temperature, and grain size. Specifically, grain sizes of 8 μm (F2: 550 mm/min, 1600 rpm) and 7.7 μm (G3: 800 mm/min, 1800 rpm) were achieved for room temperature specimens.

This section underscores that FSP coupled with rapid cooling is an efficacious approach for achieving ultra-fine grain refinement and consequential enhancement of mechanical properties. Recent years have witnessed a heightened research focus on utilizing diverse coolants within the FSP, including liquid CO_2, cooling oil, and brine solution. Additionally, there has been substantial discourse on grain size and texture evolution in conventional FSP.

In a study by Mosayebi et al. [197], FSP was conducted at varying traverse speeds ranging from 30 to 90 mm/min while maintaining a constant rotation speed to investigate the interplay between textural characteristics and grain growth performance of a Mg alloy subjected to FSP. The presence of the typical {0001} ⟨uvtw⟩ texture component was reported in the FSPed Mg alloy. A cold source-assisted FSP approach was employed by Xu et al. [198] on Mg alloy sheets, utilizing a rotational speed of 600 rpm and traverse speed of 400 mm/min. A liquid CO_2 cooling nozzle was positioned adjacent to the tool, synchronized with the processing speed. This configuration induced discernible impacts on the microstructure and mechanical attributes.

Furthermore, a study by Chandran et al. [199] encompassed FSP under distinct cooling media—water, brine solution, and cooling oil applied to AZ31 alloy. The investigation delved into the effects of these different cooling mediums on parameters such as hardness, percentage of elongation, and tensile strength. Notably, the study unveiled higher hardness under the coolant medium and comparatively diminished values in the water medium (as depicted in Fig. 29).

Table 8
Average grain size of CFSP under various cooling conditions.

Case	Description	Locations	Average grain (μm)
1	Cryogenic cooling underneath the fixture bottom	Bottom	0.5–2
		Middle	5–10
		Top	8–10
2	Cryogenic cooling on top as well as underneath the fixture bottom	Bottom	0.5–1
		Middle	3–5
		Top	8–10

4.3. FSP for biomedical industries

Interestingly, bio absorbable Mg and its alloys have been employed as metallic biomaterials in orthopedic implants because of their mechanical properties closely match with properties of human bones. In the development of implants, the major concern is stress shielding which could be avoided by matching the stiffness of the implants with stiffness of the bone. Titanium and Stainless steel are most used metals in orthopedic applications. But stress shielding issue is still existing with unsolved research problem. FSP stands out as a highly efficient technique for crafting bio-composites through the integration of bioactive particles into a metallic matrix [200,201]. Notably, the process of dynamic recrystallization during FSP leads to a finer grain structure within the matrix. Moreover, the severe plastic deformation applied during FSP induces the fragmentation and even distribution of secondary phase particles. These transformative microstructural alterations significantly enhance the characteristics of bioabsorbable Mg alloys [202,203].

In a study conducted by Mehdizade et al. [204], wollastonite ($CaSiO_3$) was utilized as a bioactive particle to create Mg-based bio--composites through the FSP method. Fig. 30 illustrates the technique used to integrate the biomaterial with the Mg alloy during the FSP process. The researchers found that the ultimate compression strength of the Mg matrix was significantly enhanced by applying six passes of FSP and incorporating wollastonite bio-ceramic particles. This improvement was attributed to the grain refinement of the Mg matrix, as well as the fragmentation and uniform redistribution of the secondary phase particles.

A study compared the properties of Mg-based biocomposites enhanced with HA and Ag particles, using FSP and coating techniques [205]. The findings demonstrated that the in-vitro biodegradation rate of the composites created via FSP was reduced by 72% compared to

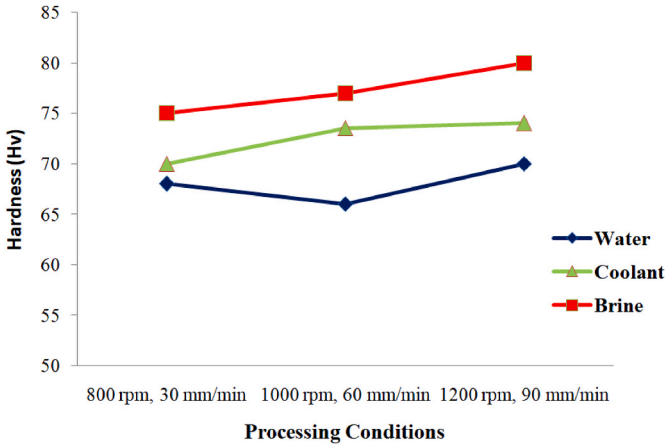

Fig. 29. Hardness of SFSP under different medium [199].

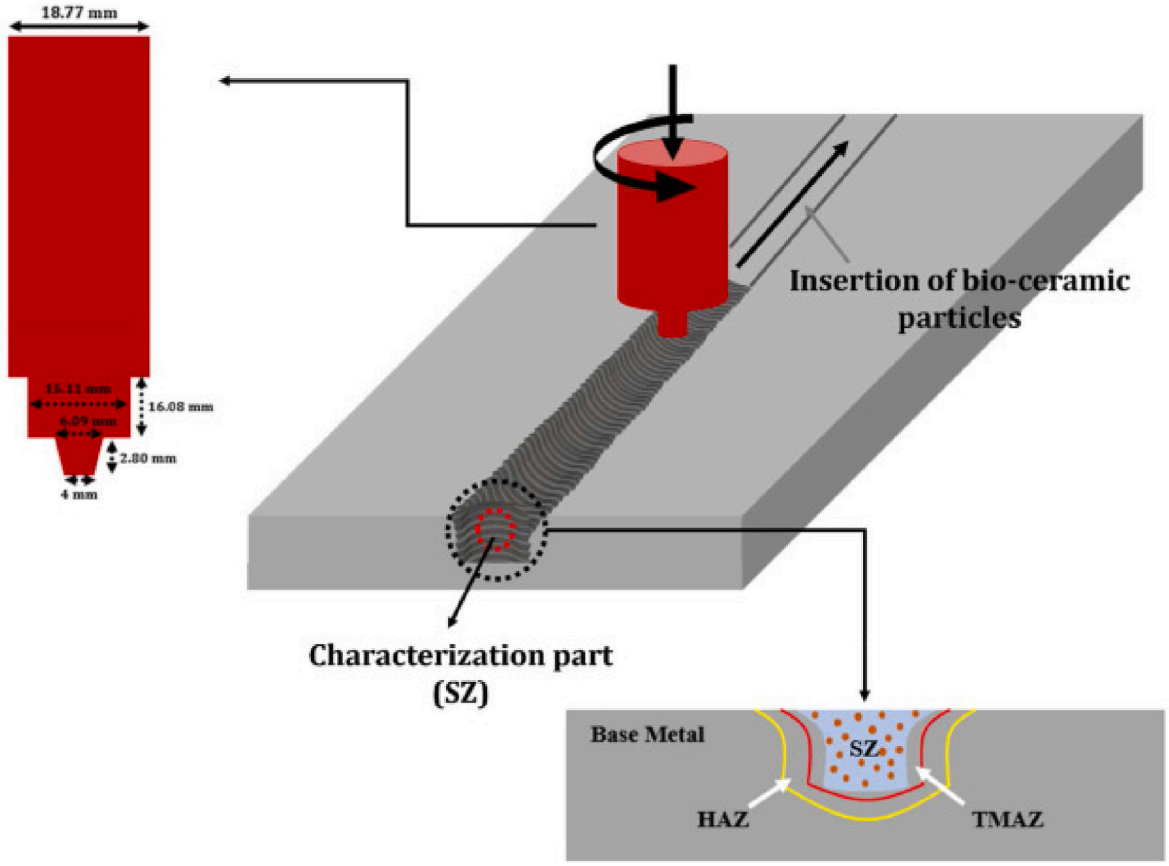

Fig. 30. Schematic representation of the fabrication process of Mg-based biocomposites via FSP [204].

those produced using the coating method. Yousefpour et al. [206] employed a multi-pass FSP method to produce AZ91/HA and AZ91/HA + Ag bio-nano composites. Their findings indicated that increasing the number of FSP passes led to greater grain refinement and more uniform dispersion of additive particles. These changes in grain refinement, texture, and dispersion of HA particles significantly improved the strength and ductility of the composites. Another research effort involved fabricating Mg-based biocomposites with the addition of HA, ZnO, and Cu/ZnO particles through the application of six passes of FSP [207]. Additionally, Thakur et al. [208] incorporated Zn and Mn micropowders into an Mg matrix, creating Mg-based biocomposites and reporting significant enhancements in the mechanical properties of the biocomposites through FSP. Kundu and Thakur [201] developed friction stir processed nano-HAp/AZ91D Mg matrix surface composite, and reported that the improved mechanical and biological performances of composites compared to the base Mg alloy. In another work, In their recent study, Shunmugasamy et al. [92] unveiled a breakthrough in orthopedic implant technology with the development of a fine-grained Mg–Zn–RE–Zr alloy. This innovative material, produced through FSP, represents a significant advancement in the field. The findings of their research showcase the remarkable potential of the processed Mg–Zn–RE–Zr alloy for facilitating osseointegration during bone tissue healing.

4.4. Friction stir additive manufacturing

Additive manufacturing (AM) stands as a transformative process, enabling the creation of objects from 3D model data through the fusion of materials using a high-energy beam as a heat source, thus layer by layer [209]. The methodology involves the melting and solidifying of successive metal layers, a technique that has revolutionized various industries [210]. However, when it comes to low-density metals such as Al and Mg alloys, traditional AM technologies face a significant challenge due to the high reflectivity of these materials. This limitation has hindered the successful AM of Al and Mg alloys using conventional methods. For solid-state AM or repair approaches, large structures were directly manufactured via wire-based friction stir additive manufacturing (W-FSAM) without kissing bonds induced by interfacial alternations. Microstructures in the deposited layers were characterized as uniform, fine and equiaxed grains. The main grain refinement mechanism involves dynamic recrystallization, which is primarily related to severe plastic deformation during the repeated stirring of thermo-plasticized materials [211,212].

In particular, Mg alloys prepared using established AM techniques, such as laser cladding [213] and selective laser melting [214], have exhibited certain drawbacks, primarily manifested in solidification flaws. Furthermore, the resulting metallic structures have displayed suboptimal static and dynamic mechanical properties [215], indicating a need for innovation in this domain. Emerging as a novel solution to address the shortcomings of conventional manufacturing approaches, Friction stir processing additive manufacturing (FSPAM) has garnered attention. This innovative technique is tailored explicitly for fabricating robust bulk Mg surface composites. The paramount objective of FSPAM is to transcend the limitations of traditional manufacturing techniques, ushering in improved mechanical properties and creating a densely packed, residual-free microstructure [216].

Conceptually derived from FSW/FSP, FSPAM deploys a non-consumable rotating tool. As it traverses along a substrate, this tool generates frictional heat and exerts intense shear stresses, leading to the plasticization of the material. Situated at the core of the tool is a mechanism for extruding solid or discontinuous feedstock. This extrusion occurs in precise alignment with designated process parameters, either above the substrate or atop the preceding layer [217,218]. FSPAM technology is shown in Fig. 31.

The evolution of the microstructure in FSPAM can be understood through a tripartite process. The initial phase involves preheating as the material exits the tool head, wherein the material's temperature experiences a notable increase owing to heat conduction emanating from the material-substrate interface. During the subsequent deposition phase, the material undergoes compression and shearing at elevated temperatures, with peak temperatures typically hovering between 0.5 and 0.9 of the material's melting point [220,221]. This intricate interplay of thermal dynamics and material manipulation constitutes the foundation of FSPAM, leading to its distinctive capacity for creating enhanced Mg alloys through advanced AM principles.

The field of FSPAM for Mg alloys has, thus far, been relatively underexplored concerning the comprehensive investigation of diverse process variables. While this realm exhibits a burgeoning potential, the research landscape is characterized by a scarcity of studies delving into the multifaceted effects of varying process parameters. Nonetheless, notable contributions have begun illuminating the promise of FSPAM for Mg alloys.

In a pivotal study by Kandasamy et al. [222], the FSPAM technique was harnessed to fabricate bulk AZ31 Mg alloy from powdered feedstock. This seminal research not only underscored the viability of FSPAM in generating defect-free and densely structured bulk Mg alloys but also illuminated its potential for inducing severe plastic deformation in the alloy. A remarkable outcome of this endeavour was the conspicuous refinement of grains within the material, characterizing a hallmark microstructure intrinsic to the FSP methodology. Joshi et al. [223] embarked on a complementary exploration into the realm of FSPAM, centering their investigation on the AZ31-B Mg alloy. With a keen focus on elucidating the intricate interplay of process parameters, their study delved into the effects of pivotal variables such as tool linear velocity, deposition material feed rate, tool residence time, and feed material deposition time. By meticulously dissecting these factors, authors unveiled a nuanced understanding of the resultant microstructure, phase composition, and crystallographic texture. A striking observation emerged from their work, revealing that the feed material (AZ31B) and the additively produced samples exhibited a shared α-Mg phase. Notably, the additively produced samples distinguished themselves through an equalized grain structure, a manifestation attributed to the fortification of the basal crystallographic texture.

While the landscape of FSPAM for Mg alloys remains in its formative stages, these pivotal studies by Kandasamy et al. [222] and Joshi et al. [223] mark crucial milestones in advancing our comprehension of this burgeoning technology's potential. Their inquiries into process variables, material behaviour, and resulting microstructures provide a solid foundation for further explorations, potentially unravelling new avenues for engineering enhanced Mg alloys via FSPAM.

5. Summary and future perspectives

This comprehensive review has provided an insightful analysis of current trends and advancements in FSP across diverse coolant mediums. FSP emerges as a compelling method for improving the properties of Mg alloys, serving as an effective surface modification technique. The complex interplay of cooling and heating within the FSP thermal cycle significantly influences the resulting grain structure and material properties, emphasizing the importance of well-engineered thermal

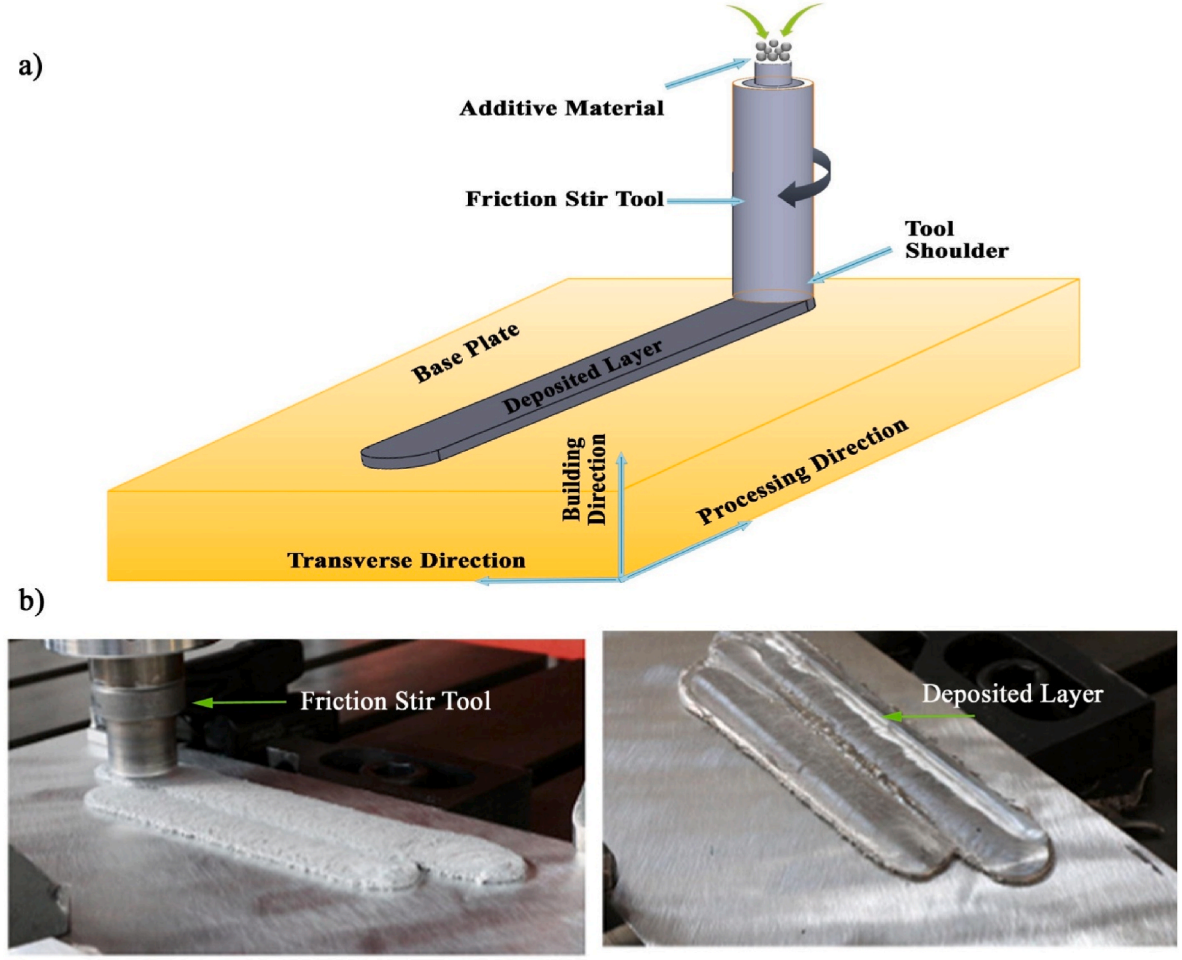

Fig. 31. a) Schematic of FSPAM technology and b) Processing method of friction surfacing layer deposition [219].

processes for optimising Mg alloy performance.

Utilizing FSP in underwater environments has led to notable enhancements in mechanical properties, grain size, corrosion resistance, and wear resistance of Mg alloys. This promising research direction holds the potential to revolutionise Mg-based component materials. The synthesis of knowledge from previous investigations indicates that cryogenic FSP shows promise for applications in cold climates, particularly in automotive and aerospace sectors where increased hardness is advantageous. However, the higher manufacturing cost of cryogenic FSP compared to SFSP underscores the importance of aligning coolant medium choice with regional requirements. SFSP offers a cost-effective option, especially in equatorial regions, while cryogenic FSP provides compelling performance advantages in specific contexts. Furthermore, FSPAM shows potential application in Mg composites, warranting further research. This comprehensive review highlights the diverse research avenues and progress within FSP, emphasizing the importance of tailoring FSP methodologies to suit varying geographical and economic considerations. As advancements continue, FSP's role in enhancing Mg alloy properties is poised to impact diverse industrial sectors significantly.

By addressing future research directions and challenges in this article, we deem the researchers would unlock new opportunities and ultimately drive innovations in materials science. Suggested some of the future works are.

i. Numerical studies on textural evolution: There is a notable gap in numerical investigations concerning to the textural evolution of FSPed Mg alloys. A comprehensive exploration of this aspect could provide valuable insights into the microstructural development and mechanical properties of FSPed materials. Continuous dynamic recrystallization (CDRX) phenomena during FSP is to be delved. Understanding governing mechanism of CDRX and its impact on the resulted microstructure would be a pivotal for optimising FSP parameters and fostering the development of high-performance Mg alloys.
ii. Study of novel coolant materials: Experimental investigations employing innovative coolant materials, particularly sustainable coolants hold significant promise for achieving nano-fine grain structures in FSPed Mg alloys. Novel coolant formulations, such as nanofluids or cryogenic fluids, could enhance heat dissipation rate and facilitate finer-grain formation. The experiments could potentially yield tailored cooling strategies, improved mechanical properties and performance of FSPed Mg alloys.
iii. Development of predictive models: It is imperative to create predictive models capable of accurately estimating heat generation and material flow during FSP. This investigation would broadcast optimum process parameters and the respective microstructural characteristics. This is one of the good research areas to explore, because optimising process parameters and predicting resultant microstructural characteristics is essential for productivity.
iv. Strategies for friction stir additive manufacturing: Combination of FSP and AM is a cutting-edge technology that leverages the advantages of both techniques to produce advanced materials with tailored properties. In this integrated approach, instead of relying solely on the layer-by-layer deposition of build materials, strategic refinement and enhanced material properties can be obtained. The further research on the best strategy in utilizing the supremacy of FSP and AM is warranted.

Funding Information

This work was supported by CERVIE, UCSI University under REIG grant, REIG-FETBE-2022/018.

Data availability

The data that support the findings of this study are available from the corresponding author upon reasonable request.

Ethical approval

This article does not contain any studies with human participants or animals performed by any authors.

Declaration of competing interest

The authors declare that they have no known competing financial interests or personal relationships that could have appeared to influence the work reported in this paper.

References

[1] Sampath B, Haribalaji V. Influences of welding parameters on friction stir welding of aluminum and magnesium: a review. Mater Res Proc 2021;19:222–30. https://doi.org/10.21741/9781644901618-28.
[2] Tesař K, Somekawa H, Singh A. Development of texture and grain size during extrusion of ZA63 alloy containing stable quasicrystalline i-phase and its effect on tensile and compression strength. J Alloys Compd 2020;849. https://doi.org/10.1016/j.jallcom.2020.156340.
[3] Zheng T-J, Zhang L-X, Liao J. Mechanical behavior and constitutive modeling of magnesium alloy sheet in ultrasonic vibration assisted tensile test. Suxing Gongcheng Xuebao/Journal Plast Eng 2020;27:170–6. https://doi.org/10.3969/j.issn.1007-2012.2020.12.024.
[4] Tan J, Ramakrishna S. Applications of magnesium and its alloys: a review. Appl Sci 2021;11. https://doi.org/10.3390/app11156861.
[5] Chen J, Tan L, Yu X, Etim IP, Ibrahim M, Yang K. Mechanical properties of magnesium alloys for medical application: a review. J Mech Behav Biomed Mater 2018;87:68–79. https://doi.org/10.1016/j.jmbbm.2018.07.022.
[6] Survey USG. Mineral commodity summaries 2020. 2020. https://doi.org/10.3133/mcs2020. Reston, vol. A.
[7] Jasinski SM. Potash. Min Eng 2011;63:91–2.
[8] Luo AA. Magnesium casting technology for structural applications. J Magnes Alloy 2013;1:2–22. https://doi.org/10.1016/j.jma.2013.02.002.
[9] Azevedo CR, Hippert E, Spera G, Gerardi P. Aircraft landing gear failure: fracture of the outer cylinder lug. Eng Fail Anal 2002;9:1–15. https://doi.org/10.1016/S1350-6307(00)00039-X.
[10] 535.0, A535.0, and B535.0: Al-Mg high-strength casting alloy. Prop. Sel. Alum. Alloy. ASM International; 2019. https://doi.org/10.31399/asm.hb.v02b.a0006585.
[11] Powell BR, Krajewski PE, Luo AA. Chapter 4 - magnesium alloys for lightweight powertrains and automotive structures. In: Mallick PK, editor. Mater. Des. Manuf. Light. Veh.. second ed. second ed. Woodhead Publishing; 2021. p. 125–86. https://doi.org/10.1016/B978-0-12-818712-8.00004-5.
[12] Asgari H, Szpunar JA, Odeshi AG, Zeng LJ, Olsson E. Experimental and simulation analysis of texture formation and deformation mechanism of rolled AZ31B magnesium alloy under dynamic loading. Mater Sci Eng A 2014;618:310–22. https://doi.org/10.1016/j.msea.2014.09.043.
[13] Guo P, Li L, Liu X, Ye T, Cao S, Xu C, et al. Compressive deformation behavior and microstructure evolution of AM80 magnesium alloy under quasi-static and dynamic loading. Int J Impact Eng 2017;109:112–20. https://doi.org/10.1016/j.ijimpeng.2017.06.004.
[14] Zhang G, Qin S, Yan L, Zhang X. Simultaneous improvement of electromagnetic shielding effectiveness and corrosion resistance in magnesium alloys by electropulsing. Mater Charact 2021;174:111042. https://doi.org/10.1016/j.matchar.2021.111042.
[15] Rahman M, Li Y, Wen C. HA coating on Mg alloys for biomedical applications: a review. J Magnes Alloy 2020;8:929–43. https://doi.org/10.1016/j.jma.2020.05.003.
[16] Tian P, Liu X. Surface modification of biodegradable magnesium and its alloys for biomedical applications. Regen Biomater 2015;2:135–51. https://doi.org/10.1093/rb/rbu013.
[17] Kappes M, Iannuzzi M, Carranza RM. Hydrogen Embrittlement of magnesium and magnesium alloys: a review. J Electrochem Soc 2013;160:C168. https://doi.org/10.1149/2.023304jes.
[18] Yang Y, Xiong X, Chen J, Peng X, Chen D, Pan F. Research advances of magnesium and magnesium alloys worldwide in 2022. J Magnes Alloy 2023. https://doi.org/10.1016/j.jma.2023.07.011.
[19] Rahim SA, Joseph MA, Sampath Kumar TS, T H. Recent progress in surface modification of Mg alloys for biodegradable orthopedic applications. Front Mater 2022;9. https://doi.org/10.3389/fmats.2022.848980.
[20] Strzelecka M, Iwaszko J, Malik M, Tomczyński S. Surface modification of the AZ91 magnesium alloy. Arch Civ Mech Eng 2015;15:854–61. https://doi.org/10.1016/j.acme.2015.03.004.

[21] Amanov A, Penkov OV, Pyun Y-S, Kim D-E. Effects of ultrasonic nanocrystalline surface modification on the tribological properties of AZ91D magnesium alloy. Tribol Int 2012;54:106–13. https://doi.org/10.1016/j.triboint.2012.04.024.
[22] Yang J, Cui F, Lee IS. Surface modifications of magnesium alloys for biomedical applications. Ann Biomed Eng 2011;39:1857–71. https://doi.org/10.1007/s10439-011-0300-y.
[23] Suresh S, Natarajan E, Mohan DG, Ang CK, Sudhagar S. Depriving friction stir weld defects in dissimilar aluminum lap joints. Proc Inst Mech Eng Part E J Process Mech Eng 2024;0:09544089241239817. https://doi.org/10.1177/09544089241239817.
[24] Manroo SA, Khan NZ, Ahmad B. Study on surface modification and fabrication of surface composites of magnesium alloys by friction stir processing: a review. J Eng Appl Sci 2022;69:25. https://doi.org/10.1186/s44147-022-00073-9.
[25] Daroonparvar M, Bakhsheshi-Rad HR, Saberi A, Razzaghi M, Kasar AK, Ramakrishna S, et al. Surface modification of magnesium alloys using thermal and solid-state cold spray processes: challenges and latest progresses. J Magnes Alloy 2022;10:2025–61. https://doi.org/10.1016/j.jma.2022.07.012.
[26] Meng X, Huang Y, Cao J, Shen J, dos Santos JF. Recent progress on control strategies for inherent issues in friction stir welding. Prog Mater Sci 2021;115:100706. https://doi.org/10.1016/j.pmatsci.2020.100706.
[27] Xie Y, Meng X, Li Y, Mao D, Wan L, Huang Y. Insight into ultra-refined grains of aluminum matrix composites via deformation-driven metallurgy. Compos Commun 2021;26:100776. https://doi.org/10.1016/j.coco.2021.100776.
[28] Mishra RS, Ma ZY, Charit I. Friction stir processing: a novel technique for fabrication of surface composite. Mater Sci Eng A 2003;341:307–10. https://doi.org/10.1016/S0921-5093(02)00199-5.
[29] Ma ZY. Friction stir processing technology: a review. Metall Mater Trans A 2008;39:642–58. https://doi.org/10.1007/s11661-007-9459-0.
[30] S S, Natarajan E, Shanmugam R, K V, N S, A A. Strategized friction stir welded AA6061-T6/SiC composite lap joint suitable for sheet metal applications. J Mater Res Technol 2022;21:30–9. https://doi.org/10.1016/j.jmrt.2022.09.022.
[31] Singh B, Singh J, Joshi RS, Singh S. Magnesium matrix composites by FSP-A review. AIP Conf Proc 2023;2800:20087. https://doi.org/10.1063/5.0163072.
[32] Zass K, Mabuwa S, Msomi V. A review on reinforced particles used on the production of FSP composites. Mater Today Proc 2022;56:2392–7. https://doi.org/10.1016/j.matpr.2021.12.210.
[33] Hu S, Wang K, Ma S, Qi H, He N, Li F. Effects of heat treatment on the interface microstructure and mechanical properties of friction-stir-processed AlCoCrFeNi/A356 composites. Materials 2023;16. https://doi.org/10.3390/ma16062234.
[34] Mirzadeh H. Surface metal-matrix composites based on AZ91 magnesium alloy via friction stir processing: a review. Int J Miner Metall Mater 2023;30:1278–96. https://doi.org/10.1007/s12613-022-2589-y.
[35] Jana S, Mishra RS, Baumann JA, Grant G. Effect of process parameters on abnormal grain growth during friction stir processing of a cast Al alloy. Mater Sci Eng A 2010;528:189–99. https://doi.org/10.1016/j.msea.2010.08.049.
[36] Salehi M, M S, J AM. Optimization of process parameters for producing AA6061/SiC nanocomposites by friction stir processing. Trans Nonferrous Met Soc China 2012;22:1055–63. https://doi.org/10.1016/S1003-6326(11)61283-1.
[37] Zoalfakar SH, Mohamed MA, Hamid MA, Megahed AA. Effect of friction stir processing parameters on producing AA6061/tungsten carbide nanocomposite. Proc Inst Mech Eng Part E J Process Mech Eng 2022;236:653–67. https://doi.org/10.1177/09544089221083558.
[38] Kundurti SC, Sharma A, Tambe P, Kumar A. Fabrication of surface metal matrix composites for structural applications using friction stir processing – a review. Mater Today Proc 2022;56:1468–77. https://doi.org/10.1016/j.matpr.2021.12.337.
[39] Mehdi H, Mehmood A, Chinchkar A, Hashmi AW, Malla C, Mohapatra P. Optimization of process parameters on the mechanical properties of AA6061/Al2O3 nanocomposites fabricated by multi-pass friction stir processing. Mater Today Proc 2022;56:1995–2003. https://doi.org/10.1016/j.matpr.2021.11.333.
[40] Hu Y, Sun Y, He J, Fang D, Zhu J, Meng X. Effect of friction stir processing parameters on the microstructure and properties of ZK60 magnesium alloy. Mater Res Express 2022;9:016508. https://doi.org/10.1088/2053-1591/ac475e.
[41] Suresh S, Venkatesan K, Natarajan E, Rajesh S, Lim WH. Evaluating weld properties of conventional and swept friction stir spot welded 6061-T6 aluminium alloy. Mater Express 2019;9:851–60. https://doi.org/10.1166/mex.2019.1584.
[42] Muthukumar P, Jerome S, Periasamy K, Raja P. Effectuates of direct particle injection friction stir process tool for the Al/SiC surface coating fabrication. Mater Today Proc 2023;90:188–91. https://doi.org/10.1016/j.matpr.2023.05.667.
[43] Vasava A, Singh D. Influence of various tool shoulder design on hybrid surface composite of AA7075-T651/SiC/graphene through friction stir processing. Can Metall Q 2023:1–19. https://doi.org/10.1080/00084433.2023.2193500. 0.
[44] Choi H, Koç M, Ni J. A study on Warm Hydroforming of Al and Mg sheet materials: mechanism and proper temperature conditions. J Manuf Sci Eng 2008;130:41007. https://doi.org/10.1115/1.2951945.
[45] Suresh S, Natarajan E, Vinayagamurthi P, Venkatesan K, Viswanathan R, Rajesh S. Optimum tool traverse speed resulting equiaxed recrystallized grains and high mechanical strength at swept friction stir spot welded AA7075-T6 lap joints. In: Natarajan E, Vinodh S, Rajkumar V, editors. Mater. Des. Manuf. Sustain. Environ. Singapore: Springer Nature Singapore; 2023. p. 547–55. https://doi.org/10.1007/978-981-19-3053-9_41.
[46] Bhojak Vishal, Jain Jinesh Kumar, Saxena Kuldeep Kumar, Singh Bharat, Mohammed KA. Friction stir process: a comprehensive review on material and methodology. Indian J Eng Mater Sci 2023;30. https://doi.org/10.56042/ijems.v1i1.61877.
[47] Suresh S, Venkatesan K, Rajesh S. Optimization of process parameters for friction stir spot welding of AA6061/Al2O3 by Taguchi method. AIP Conf Proc 2019;2128:030018. https://doi.org/10.1063/1.5117961.
[48] Suresh S, Natarajan E, Franz G, Rajesh S. Differentiation in the SiC filler size effect in the mechanical and tribological properties of friction-spot-welded AA5083-H116 alloy. Fibers 2022;10:109. https://doi.org/10.3390/fib10120109.
[49] Sandeep KJ, Choudhary AK, Immanuel RJ. Microstructural characterization and mechanical performance of AZ91 magnesium alloy processed by friction stir processing using novel tool designs. J Mater Eng Perform 2023. https://doi.org/10.1007/s11665-023-07980-9.
[50] Boopathi S, V HB, Mageswari M, Asif MM. Influences of boron carbide particles on the wear rate and tensile strength of AA2014 surface composite fabricated by friction-stir processing. Mater Tehnol 2022;56. https://doi.org/10.17222/mit.2022.409.
[51] Zheng FY, Wu YJ, Peng LM, Li XW, Fu PH, Ding WJ. Microstructures and mechanical properties of friction stir processed Mg–2.0Nd–0.3Zn–1.0Zr magnesium alloy. J Magnes Alloy 2013;1:122–7. https://doi.org/10.1016/j.jma.2013.06.001.
[52] Samanta A, Das H, Grant GJ, Jana S. Effect of tool design and pass strategy on defect elimination and uniform, enhanced tensile properties of friction stir processed high-pressure die-cast A380 alloy. Mater Sci Eng A 2022;861:144388. https://doi.org/10.1016/j.msea.2022.144388.
[53] Panaskar NJ, Sharma A. Surface modification and nanocomposite layering of Fastener-Hole through friction-stir processing. Mater Manuf Process 2014;29:726–32. https://doi.org/10.1080/10426914.2014.892619.
[54] Langlade C, Roman A, Schlegel D, Gete E, Noel P, Folea M. Influence of friction stir process parameters on surface quality of aluminum alloy A2017. MATEC Web Conf 2017;94:2006. https://doi.org/10.1051/matecconf/20179402006.
[55] Ku M-H, Hung F-Y, Lui T-S. Embrittlement due to excess heat input into friction stir processed 7075 alloy. Mater (Basel, Switzerland) 2019;12. https://doi.org/10.3390/ma12020227.
[56] Chintalu RS, Padmanaban R, Vignesh RV. Finite element modelling of thermal history during friction stir processing of AA5052. Mater Today Proc 2021;46:7452–8. https://doi.org/10.1016/j.matpr.2021.01.105.
[57] Leszczyńska-Madej B, Hrabia-Wiśnios J, Węglowska A, Perek-Nowak M, Madej M. Experimental investigations of heat generation and microstructure evolution during friction stir processing of SnSbCu alloy. Arch Civ Mech Eng 2022;22:202. https://doi.org/10.1007/s43452-022-00530-5.
[58] Węglowski MS. Friction stir processing – state of the art. Arch Civ Mech Eng 2018;18:114–29. https://doi.org/10.1016/j.acme.2017.06.002.
[59] Bhojak V, Jain JK, Singhal TS, Saxena KK, Prakash C, Agrawal MK, et al. Friction stir processing and cladding: an innovative surface engineering technique to tailor magnesium-based alloys fFor biomedical implants. Surf Rev Lett 2023;0:2340007. https://doi.org/10.1142/S0218625X23400073.
[60] Suganeswaran K, Ragu Nathan S, Parameshwaran R, Nithyavathy N, Dhineshbabu NR. Characterization of AA7075 surface composites with ex situ Al2O3/SiC reinforcements tailored using friction stir processing. J Mater Eng Perform 2023;32:3617–32. https://doi.org/10.1007/s11665-022-07354-7.
[61] Rafi SM, Satish Kumar T, Thankachan T, Selvan CP. Synergistic effect of FSP and TiB2 on mechanical and tribological behavior of AA2024 surface composites. J Tribol 2023;145. https://doi.org/10.1115/1.4062517.
[62] Kumar S. Ultrasonic assisted friction stir processing of 6063 aluminum alloy. Arch Civ Mech Eng 2016;16:473–84. https://doi.org/10.1016/j.acme.2016.03.002.
[63] Padhy GK, Wu CS, Gao S. Auxiliary energy assisted friction stir welding – status review. Sci Technol Weld Join 2015;20:631–49. https://doi.org/10.1179/1362171815Y.0000000048.
[64] Pan L, Kwok CT, Lo KH. Effect of multiple-pass friction stir processing on hardness and corrosion resistance of martensitic stainless steel. Coatings 2019;9. https://doi.org/10.3390/coatings9100620.
[65] Patel M, Chaudhary B, Murugesan J, Jain NK, Patel V. Enhancement of tensile and fatigue properties of hybrid aluminium matrix composite via multipass friction stir processing. J Mater Res Technol 2022;21:4811–23. https://doi.org/10.1016/j.jmrt.2022.11.073.
[66] Ingarao G, Baffari D, Bracquené E, Fratini L, Duflou J. Energy demand reduction of aluminum alloys recycling through friction stir extrusion processes implementation. Procedia Manuf 2019;33:632–8. https://doi.org/10.1016/j.promfg.2019.04.079.
[67] Baffari D, Buffa G, Campanella D, Fratini L, Reynolds AP. Process mechanics in Friction Stir Extrusion of magnesium alloys chips through experiments and numerical simulation. J Manuf Process 2017;29:41–9. https://doi.org/10.1016/j.jmapro.2017.07.010.
[68] Wang Q, Zhao Z, Zhao Y, Yan K, Zhang H. The adjustment strategy of welding parameters for spray formed 7055 aluminum alloy underwater friction stir welding joint. Mater Des 2015;88:1366–76. https://doi.org/10.1016/j.matdes.2015.09.038.
[69] Trojovský P, Dhasarathan V, Boopathi S. Experimental investigations on cryogenic friction-stir welding of similar ZE42 magnesium alloys. Alexandria Eng J 2023;66:1–14. https://doi.org/10.1016/j.aej.2022.12.007.
[70] Jeong Y-H, Hossain MAM, Hong S-T, Han K-S, Lee K-J, Park J-W, et al. Effects of friction stir processing on the thermal conductivity of a strain-hardened Al-Mg alloy. Int J Precis Eng Manuf 2015;16:1969–74. https://doi.org/10.1007/s12541-015-0256-1.
[71] del Valle JA, Rey P, Gesto D, Verdera D, Jiménez JA, Ruano OA. Mechanical properties of ultra-fine grained AZ91 magnesium alloy processed by friction stir processing. Mater Sci Eng A 2015;628:198–206. https://doi.org/10.1016/j.msea.2015.01.030.

[72] Zang Q, Chen H, Lan F, Zhang J, Jin Y. Effect of friction stir processing on microstructure and damping capacity of AZ31 alloy. J Cent South Univ 2017;24:1034–9. https://doi.org/10.1007/s11771-017-3506-9.
[73] Raja A, Biswas P, Pancholi V. Effect of layered microstructure on the superplasticity of friction stir processed AZ91 magnesium alloy. Mater Sci Eng A 2018;725:492–502. https://doi.org/10.1016/j.msea.2018.04.028.
[74] Md FK, Panigrahi SK. Achieving excellent superplasticity in an ultrafine-grained QE22 alloy at both high strain rate and low-temperature regimes. J Alloys Compd 2018;747:71–82. https://doi.org/10.1016/j.jallcom.2018.02.294.
[75] Shang Q, Ni DR, Xue P, Xiao BL, Wang KS, Ma ZY. An approach to enhancement of Mg alloy joint performance by additional pass of friction stir processing. J Mater Process Technol 2019;264:336–45. https://doi.org/10.1016/j.jmatprotec.2018.09.021.
[76] Zhang Z, Li Y, Peng J, Guo P, Huang J, Yang P, et al. Combining surface mechanical attrition treatment with friction stir processing to optimize the mechanical properties of a magnesium alloy. Mater Sci Eng A 2019;756:184–9. https://doi.org/10.1016/j.msea.2019.04.051.
[77] Vasua C, Venkateswarlub B, Raoa RV, Chantia B, Saikrishnaa M, Sunil BR. Microstructure, mechanical and corrosion properties of friction stir processed ZE41 Mg alloy. Mater Today Proc 2019;15:50–6. https://doi.org/10.1016/j.matpr.2019.05.023.
[78] Peng J, Zhang Z, Huang J, Guo P, Li Y, Zhou W, et al. The effect of the inhomogeneous microstructure and texture on the mechanical properties of AZ31 Mg alloys processed by friction stir processing. J Alloys Compd 2019;792:16–24. https://doi.org/10.1016/j.jallcom.2019.04.014.
[79] Jin Y, Wang K, Wang W, Peng P, Zhou S, Huang L, et al. Microstructure and mechanical properties of AE42 rare earth-containing magnesium alloy prepared by friction stir processing. Mater Charact 2019;150:52–61. https://doi.org/10.1016/j.matchar.2019.02.008.
[80] Luo XC, Zhang DT, Cao GH, Qiu C, Chen DL. High-temperature tensile behavior of AZ61 magnesium plate prepared by multi-pass friction stir processing. Mater Sci Eng A 2019;759:234–40. https://doi.org/10.1016/j.msea.2019.05.050.
[81] Seifiyan H, Heydarzadeh Sohi M, Ansari M, Ahmadkhaniha D, Saremi M. Influence of friction stir processing conditions on corrosion behavior of AZ31B magnesium alloy. J Magnes Alloy 2019;7:605–16. https://doi.org/10.1016/j.jma.2019.11.004.
[82] Fashami HAA, Arab NBM, Gollo MH, Nami B. Effect of multi-pass friction stir processing on thermal distribution and mechanical properties of AZ91. Mech Ind 2020;21. https://doi.org/10.1051/meca/2020042.
[83] Singh Sidhu H, Singh B, Kumar P. To study the corrosion behavior of friction stir processed magnesium alloy AZ91. Mater Today Proc 2020;44:4633–9. https://doi.org/10.1016/j.matpr.2020.10.920.
[84] Liu F, Ji Y, Bai Y. Influence of multipass high rotating speed friction stir processing on microstructure evolution, corrosion behavior and mechanical properties of stirred zone on AZ31 alloy. Trans Nonferrous Met Soc China 2020;30:3263–73. https://doi.org/10.1016/S1003-6326(20)65459-0.
[85] Babu B, Babu A, Janardhana R. Tailoring ZE41 Mg alloy by friction stir processing for biomedical applications: role of microstructure on the degradation and mechanical behavior in Simulated body fluids. Trans Indian Inst Met 2020;73:2889–99. https://doi.org/10.1007/s12666-020-02090-9.
[86] Patel V, Li W, Liu X, Wen Q, Su Y, Shen J, et al. Tailoring grain refinement through thickness in magnesium alloy via stationary shoulder friction stir processing and copper backing plate. Mater Sci Eng A 2020;784. https://doi.org/10.1016/j.msea.2020.139322.
[87] Luo XC, Kang LM, Liu HL, Li ZJ, Liu YF, Zhang DT, et al. Enhancing mechanical properties of AZ61 magnesium alloy via friction stir processing: effect of processing parameters. Mater Sci Eng A 2020;797:139945. https://doi.org/10.1016/j.msea.2020.139945.
[88] Kumar A, Gotawala N, Mishra S, Shrivastava A. Defects, microstructure and mechanical behaviour upon multi-pass friction stir processing of magnesium alloy with spiral tool path. CIRP J Manuf Sci Technol 2021;32:170–8. https://doi.org/10.1016/j.cirpj.2020.12.006.
[89] Wu B, Yusof F, Li F, Abdul Razak BB, Bin Muhamad MR, Badruddin IA, et al. Influence of friction stir processing parameters on microstructure, hardness and corrosion resistance of biocompatible Mg alloy WE43. Arab J Sci Eng 2023. https://doi.org/10.1007/s13369-023-08037-8.
[90] Zheng T, Hu Y, Zhang C, Zhao T, Jiang B, Pan F, et al. Uncovering of the formation of rare earth texture and pseudo fiber bimodal microstructure in the high ductility Mg-2Gd-0.4Zr alloy during extrusion. J Mater Sci Technol 2024;172:166–84. https://doi.org/10.1016/j.jmst.2023.06.055.
[91] Yu Z, Xu X, Shi K, Du B, Han X, Xiao T, et al. Development and characteristics of a low rare-earth containing magnesium alloy with high strength-ductility synergy. J Magnes Alloy 2023;11:1629–42. https://doi.org/10.1016/j.jma.2022.01.005.
[92] Shunmugasamy VC, AbdelGawad M, Sohail MU, Ibrahim T, Khan T, Seers TD, et al. In vitro and in vivo study on fine-grained Mg–Zn–RE–Zr alloy as a biodegradeable orthopedic implant produced by friction stir processing. Bioact Mater 2023;28:448–66. https://doi.org/10.1016/j.bioactmat.2023.06.010.
[93] Manjhi SK, Sekar P, Bontha S, Balan ASS. Additive manufacturing of magnesium alloys: characterization and Postprocessing. Int J Light Mater Manuf 2023. https://doi.org/10.1016/j.ijlmm.2023.06.004.
[94] Lü Y, Wang Q, Zeng X, Ding W, Zhai C, Zhu Y. Effects of rare earths on the microstructure, properties and fracture behavior of Mg–Al alloys. Mater Sci Eng A 2000;278:66–76. https://doi.org/10.1016/S0921-5093(99)00604-8.
[95] Fan JF, Yang CL, Han G, Fang S, Yang WD, Xu BS. Oxidation behavior of ignition-proof magnesium alloys with rare earth addition. J Alloys Compd 2011;509:2137–42. https://doi.org/10.1016/j.jallcom.2010.10.168.
[96] Liu F, Ma ZY, Tan MJ. Facilitating basal slip to increase deformation Ability in Mg-Mn-Ce alloy by textural Reconstruction using friction stir processing. Metall Mater Trans A 2013;44:3947–60. https://doi.org/10.1007/s11661-013-1746-3.
[97] Xin R, Zheng X, Liu Z, Liu D, Qiu R, Li Z, et al. Microstructure and texture evolution of an Mg–Gd–Y–Nd–Zr alloy during friction stir processing. J Alloys Compd 2016;659:51–9. https://doi.org/10.1016/j.jallcom.2015.11.034.
[98] Yang Q, Feng AH, Xiao BL, Ma ZY. Influence of texture on superplastic behavior of friction stir processed ZK60 magnesium alloy. Mater Sci Eng A 2012;556:671–7. https://doi.org/10.1016/j.msea.2012.07.046.
[99] Xie GM, Ma ZY, Geng L, Chen RS. Microstructural evolution and enhanced superplasticity in friction stir processed Mg–Zn–Y–Zr alloy. J Mater Res 2008;23:1207–13. https://doi.org/10.1557/JMR.2008.0164.
[100] Luo ZA, Xie GM, Ma ZY, Wang GL, Wang GD. Effect of Yttrium addition on microstructural characteristics and superplastic behavior of friction stir processed ZK60 alloy. J Mater Sci Technol 2013;29:1116–22. https://doi.org/10.1016/j.jmst.2013.10.031.
[101] Yang Q, Xiao BL, Ma ZY. Enhanced superplasticity in friction stir processed Mg–Gd–Y–Zr alloy. J Alloys Compd 2013;551:61–6. https://doi.org/10.1016/j.jallcom.2012.10.002.
[102] Freeney TA, Mishra RS. Effect of friction stir processing on microstructure and mechanical properties of a cast-magnesium–rare earth alloy. Metall Mater Trans A 2010;41:73–84. https://doi.org/10.1007/s11661-009-0080-2.
[103] Yang Q, Xiao BL, Ma ZY. Influence of process parameters on microstructure and mechanical properties of friction-stir-processed Mg-Gd-Y-Zr casting. Metall Mater Trans A 2012;43:2094–109. https://doi.org/10.1007/s11661-011-1076-2.
[104] Yang Q, Xiao BL, Wang D, Zheng MY, Ma ZY. Study on distribution of long-period stacking ordered phase in Mg–Gd–Y–Zn–Zr alloy using friction stir processing. Mater Sci Eng A 2015;626:275–85. https://doi.org/10.1016/j.msea.2014.12.091.
[105] Jain V, Mishra R, Verma R, Essadiqi E. Superplasticity and microstructural stability in a Mg alloy processed by hot rolling and friction stir processing. Scr Mater 2013;68:447–50. https://doi.org/10.1016/j.scriptamat.2012.11.009.
[106] Panigrahi SK, Kumar K, Kumar N, Yuan W, Mishra RS, DeLorme R, et al. Transition of deformation behavior in an ultrafine grained magnesium alloy. Mater Sci Eng A 2012;549:123–7. https://doi.org/10.1016/j.msea.2012.04.017.
[107] Jamili AM, Zarei-Hanzaki A, Abedi HR, Minárik P, Soltani R. The microstructure, texture, and room temperature mechanical properties of friction stir processed Mg-Y-Nd alloy. Mater Sci Eng A 2017;690:244–53. https://doi.org/10.1016/j.msea.2017.02.096.
[108] Tsujikawa M, Chung SW, Morishige T, Chiang LF, Takigawa Y, Oki S, et al. Microstructural evolution of friction stir processed cast Mg-5.9 mass%Y-2.6 mass %Zn alloy in high temperature deformation. Mater Trans 2007;48:618–21. https://doi.org/10.2320/matertrans.48.618.
[109] Huang Y, Wang Y, Meng X, Wan L, Cao J, Zhou L, et al. Dynamic recrystallization and mechanical properties of friction stir processed Mg-Zn-Y-Zr alloys. J Mater Process Technol 2017;249:331–8. https://doi.org/10.1016/j.jmatprotec.2017.06.021.
[110] Morishige T, Tsujikawa M, Oki S, Kamita M, Chung SW, Higashi K. Friction stir processing of cast Mg-Y-Zn alloy. Adv Mater Res 2006;15–17:369–74. https://dx.doi.org/10.4028/www.scientific.net/AMR.15-17.369.
[111] Jamili AM, Zarei-Hanzaki A, Abedi HR, Mosayebi M, Kocich R, Kunčická L. Development of fresh and fully recrystallized microstructures through friction stir processing of a rare earth bearing magnesium alloy. Mater Sci Eng A 2020;775:138837. https://doi.org/10.1016/j.msea.2019.138837.
[112] Yousefpour F, Jamaati R, Aval HJ. Effect of traverse and rotational speeds on microstructure, texture, and mechanical properties of friction stir processed AZ91 alloy. Mater Charact 2021;178:111235. https://doi.org/10.1016/j.matchar.2021.111235.
[113] Zhang D, Wang S, Qiu C, Zhang W. Superplastic tensile behavior of a fine-grained AZ91 magnesium alloy prepared by friction stir processing. Mater Sci Eng A 2012;556:100–6. https://doi.org/10.1016/j.msea.2012.06.063.
[114] Luo XC, Zhang DT, Zhang WW, Qiu C, Chen DL. Tensile properties of AZ61 magnesium alloy produced by multi-pass friction stir processing: effect of sample orientation. Mater Sci Eng A 2018;725:398–405. https://doi.org/10.1016/j.msea.2018.04.017.
[115] Vargas M, Lathabai S, Uggowitzer PJ, Qi Y, Orlov D, Estrin Y. Microstructure, crystallographic texture and mechanical behaviour of friction stir processed Mg-Zn-Ca-Zr alloy ZKX50. Mater Sci Eng A 2017;685:253–64. https://doi.org/10.1016/j.msea.2016.12.125.
[116] Wang Y, Huang Y, Meng X, Wan L, Feng J. Microstructural evolution and mechanical properties of Mg Zn Y Zr alloy during friction stir processing. J Alloys Compd 2017;696:875–83. https://doi.org/10.1016/j.jallcom.2016.12.068.
[117] Jin Y, Wang K, Wang W, Peng P, Zhou S, Huang L, et al. Microstructure and mechanical properties of AE42 rare earth-containing magnesium alloy prepared by friction stir processing. Mater Charact 2019;150:52–61. https://doi.org/10.1016/j.matchar.2019.02.008.
[118] Liu F, Ji Y, Sun Z, Liu J, Bai Y, Shen Z. Enhancing corrosion resistance and mechanical properties of AZ31 magnesium alloy by friction stir processing with the same speed ratio. J Alloys Compd 2020;829:154452. https://doi.org/10.1016/j.jallcom.2020.154452.
[119] Liu G, Ma Z, Wei G, Xu T, Zhang X, Yang Y, et al. Microstructure, tensile properties and corrosion behavior of friction stir processed Mg-9Li-1Zn alloy. J Mater Process Technol 2019;267:393–402. https://doi.org/10.1016/j.jmatprotec.2018.12.026.
[120] Li J, Huang Y, Wang F, Meng X, Wan L, Dong Z. Enhanced strength and ductility of friction-stir-processed Mg–6Zn alloys via Y and Zr co-alloying. Mater Sci Eng A 2020;773:138877. https://doi.org/10.1016/j.msea.2019.138877.

[121] Luo X, Liu H, Kang L, Lin J, Liu Y, Zhang D, et al. Stretch formability of an AZ61 alloy plate prepared by multi-pass friction stir processing. Materials 2021;14. https://doi.org/10.3390/ma14123168.
[122] Heidarzadeh A, Mironov S, Kaibyshev R, Çam G, Simar A, Gerlich A, et al. Friction stir welding/processing of metals and alloys: a comprehensive review on microstructural evolution. Prog Mater Sci 2021;117:100752. https://doi.org/10.1016/j.pmatsci.2020.100752.
[123] Sharahi HJ, Pouranvari M, Movahedi M. Strengthening and ductilization mechanisms of friction stir processed cast Mg–Al–Zn alloy. Mater Sci Eng A 2020;781:139249. https://doi.org/10.1016/j.msea.2020.139249.
[124] Badkoobeh F, Nouri A, Hassannejad H. The bake hardening mechanism of dual-phase silicon steels under high pre-strain. Mater Sci Eng A 2020;770:138544. https://doi.org/10.1016/j.msea.2019.138544.
[125] Muga CO, Zhang ZW. Strengthening mechanisms of magnesium-Lithium based alloys and composites. Adv Mater Sci Eng 2016;2016:1078187. https://doi.org/10.1155/2016/1078187.
[126] Xiao P, Gao Y, Yang C, Li Y, Huang X, Liu Q, et al. Strengthening and toughening mechanisms of Mg matrix composites reinforced with specific spatial arrangement of in-situ TiB2 nanoparticles. Compos Part B Eng 2020;198:108174. https://doi.org/10.1016/j.compositesb.2020.108174.
[127] Singh K, Singh G, Singh H. Review on friction stir welding of magnesium alloys. J Magnes Alloy 2018;6:399–416. https://doi.org/10.1016/j.jma.2018.06.001.
[128] Bharathi BM, Vignesh RV, Padmanaban R, Govindaraju M. Effect of friction stir processing and heat treatment on the corrosion properties of AZ31 alloy. Aust J Mech Eng 2022;20:1479–88. https://doi.org/10.1080/14484846.2020.1815999.
[129] Qin D, Shen H, Shen Z, Chen H, Fu L. Manufacture of biodegradable magnesium alloy by high speed friction stir processing. J Manuf Process 2018;36:22–32. https://doi.org/10.1016/j.jmapro.2018.09.019.
[130] Huang L, Wang K, Wang W, Yuan J, Qiao K, Yang T, et al. Effects of grain size and texture on stress corrosion cracking of friction stir processed AZ80 magnesium alloy. Eng Fail Anal 2018;92:392–404. https://doi.org/10.1016/j.engfailanal.2018.06.012.
[131] Liu Q, Ma Q, Chen G, Cao X, Zhang S, Pan J, et al. Enhanced corrosion resistance of AZ91 magnesium alloy through refinement and homogenization of surface microstructure by friction stir processing. Corros Sci 2018;138:284–96. https://doi.org/10.1016/j.corsci.2018.04.028.
[132] Hassani B, Vallant R, Karimzadeh F, Enayati MH, Sabooni S, Pradeep K. Effect of friction stir processing on corrosion behavior of cast AZ91C magnesium alloy. Surf Rev Lett 2019;26:1850213. https://doi.org/10.1142/S0218625X1850213X.
[133] Huang L, Wang K, Wang W, Peng P, Qiao K, Liu Q. Microstructural evolution and corrosion behavior of friction stir processed fine-grained AZ80 Mg alloy. Mater Corros 2020;71:93–108. https://doi.org/10.1002/maco.201911108.
[134] Zhu Y, Zhou M, Geng Y, Zhang S, Xin T, Chen G, et al. Microstructural evolution and its influence on mechanical and corrosion behaviors in a high-Al/Zn containing duplex Mg-Li alloy after friction stir processing. J Mater Sci Technol 2024;184:245–55. https://doi.org/10.1016/j.jmst.2023.10.019.
[135] Liu D, Shen M, Tang Y, Hu Y, Zhao L. Effect of multipass friction stir processing on surface corrosion resistance and wear resistance of ZK60 alloy. Met Mater Int 2019;25:1–9. https://doi.org/10.1007/s12540-019-00268-5.
[136] Liu Q, Chen G, Zeng S, Zhang S, Long F, Shi Q. The corrosion behavior of Mg-9Al-xRE magnesium alloys modified by friction stir processing. J Alloys Compd 2021;851:156835. https://doi.org/10.1016/j.jallcom.2020.156835.
[137] Arora HS, Singh H, Dhindaw BK. Wear behaviour of a Mg alloy subjected to friction stir processing. Wear 2013;303:65–77. https://doi.org/10.1016/j.wear.2013.02.023.
[138] Rathinasuriyan C, Sankar R. Wear and corrosion behavior of cryogenic friction stir processed AZ31B alloy. J Mater Eng Perform 2021;30:3118–28. https://doi.org/10.1007/s11665-021-05636-0.
[139] Kumar A, Gotawala N, Mishra S, Shrivastava A. Defects, microstructure and mechanical behaviour upon multi-pass friction stir processing of magnesium alloy with spiral tool path. CIRP J Manuf Sci Technol 2021;32:170–8. https://doi.org/10.1016/j.cirpj.2020.12.006.
[140] Hütsch LL, Hütsch J, Herzberg K, dos Santos JF, Huber N. Increased room temperature formability of Mg AZ31 by high speed Friction Stir Processing. Mater Des 2014;54:980–8. https://doi.org/10.1016/j.matdes.2013.08.108.
[141] Cavaliere P, Marco PP. Friction stir processing of AM60B magnesium alloy sheets. Mater Sci Eng A-Structural Mater Prop Microstruct Process - MATER SCI ENG A-STRUCT MATER 2007;462:393–7. https://doi.org/10.1016/j.msea.2006.04.150.
[142] Venkateswarlu G, Devaraju D, Davidson MJ, Kotiveerachari B, Tagore GRN. Effect of overlapping ratio on mechanical properties and formability of friction stir processed Mg AZ31B alloy. Mater Des 2013;45:480–6. https://doi.org/10.1016/j.matdes.2012.08.031.
[143] Venkateswarlu G, Davidson DMJ, Tagore GRN. Modelling studies of sheet metal formability of friction stir processed Mg AZ31B alloy under stretch forming. Mater Des 2012;40:1–6. https://doi.org/10.1016/j.matdes.2012.03.012.
[144] Wang W, Han P, Peng P, Zhang T, Liu Q, Yuan S-N, et al. Friction stir processing of magnesium alloys: a review. Acta Metall Sin (English Lett 2020;33:43–57. https://doi.org/10.1007/s40195-019-00971-7.
[145] Ramesh Babu S, Senthil Kumar VS, Karunamoorthy L, Madhusudhan Reddy G. Investigation on the effect of friction stir processing on the superplastic forming of AZ31B alloy. Mater Des 2014;53:338–48. https://doi.org/10.1016/j.matdes.2013.07.005.
[146] Cavaliere P, De Marco PP. Superplastic behaviour of friction stir processed AZ91 magnesium alloy produced by high pressure die cast. J Mater Process Technol 2007;184:77–83. https://doi.org/10.1016/j.jmatprotec.2006.11.005.
[147] Sheng SX, Guo YL, Liu SF, Wu SL. Superplasticity Mg alloy fabricated by friction stir processing. Mater. Process. Technol. V 2014;941:93–6. Trans Tech Publications Ltd, https://dx.doi.org/10.4028/www.scientific.net/AMR.941-944.93.
[148] Zhang D, Xiong F, Zhang W, Qiu C, Zhang W. Superplasticity of AZ31 magnesium alloy prepared by friction stir processing. Trans Nonferrous Met Soc China 2011;21:1911–6. https://doi.org/10.1016/S1003-6326(11)60949-7.
[149] Takayama Y, Takeda I, Shibayanagi T, Kato H, Funami K. Superplasticity in friction stir processed AZ80 magnesium alloy. Superplast. Adv. Mater. - ICSAM 2009;433:241–6. Trans Tech Publications Ltd; 2010, https://dx.doi.org/10.4028/www.scientific.net/KEM.433.241.
[150] Kandalam S, Sabat RK, Bibhanshu N, Avadhani GS, Kumar S, Suwas S. Superplasticity in high temperature magnesium alloy WE43. Mater Sci Eng A 2017;687:85–92. https://doi.org/10.1016/j.msea.2016.12.129.
[151] Rs B. Different strategies of secondary phase incorporation into metallic sheets by friction stir processing in developing surface composites. Int J Mech Mater Eng 2016;11:12. https://doi.org/10.1186/s40712-016-0066-y.
[152] Suresh S, Venkatesan K, Natarajan E, Rajesh S. Performance analysis of nano silicon carbide reinforced swept friction stir spot weld joint in AA6061-T6 alloy. Silicon 2021;13:3399–412. https://doi.org/10.1007/s12633-020-00751-4.
[153] Suresh S, Venkatesan K, Natarajan E. Influence of SiC nanoparticle reinforcement on FSS welded 6061-T6 aluminum alloy. J Nanomater 2018;2018:1–11. https://doi.org/10.1155/2018/7031867.
[154] Suresh S, Elango N, Venkatesan K, Lim WH, Palanikumar K, Rajesh S. Sustainable friction stir spot welding of 6061-T6 aluminium alloy using improved non-dominated sorting teaching learning algorithm. J Mater Res Technol 2020;9:11650–74. https://doi.org/10.1016/j.jmrt.2020.08.043.
[155] Suresh S, Venkatesan K, Natarajan E, Rajesh S. Influence of tool rotational speed on the properties of friction stir spot welded AA7075-T6/Al2O3 composite joint. Mater Today Proc 2020;27:62–7. https://doi.org/10.1016/j.matpr.2019.08.220.
[156] Balakrishnan M, Dinaharan I, Palanivel R, Sivaprakasam R. Synthesize of AZ31/TiC magnesium matrix composites using friction stir processing. J Magnes Alloy 2015;3:76–8. https://doi.org/10.1016/j.jma.2014.12.007.
[157] Dinaharan I, Zhang S, Chen G, Shi Q. Titanium particulate reinforced AZ31 magnesium matrix composites with improved ductility prepared using friction stir processing. Mater Sci Eng A 2020;772:138793. https://doi.org/10.1016/j.msea.2019.138793.
[158] Bhadouria N, Kumar P, Thakur L, Dixit S, Arora N. A study on micro-hardness and tribological behaviour of nano-WC–Co–Cr/Multi-walled carbon Nanotubes reinforced AZ91D magnesium matrix surface composites. Trans Indian Inst Met 2017;70:2477–83. https://doi.org/10.1007/s12666-017-1111-0.
[159] Mishra M, Prakash C, Shabadi R, Singh S. Mechanical and microstructural characterization of magnesium/multi-walled carbon Nanotubes composites fabricated via friction stir processing. In: Prakash C, Singh S, Krolczyk G, Pabla BS, editors. Adv. Mater. Sci. Eng. Singapore: Springer Singapore; 2020. p. 137–47.
[160] Sunil BR, Reddy GPK, Patle H, Dumpala R. Magnesium based surface metal matrix composites by friction stir processing. J Magnes Alloy 2016;4:52–61. https://doi.org/10.1016/j.jma.2016.02.001.
[161] Chelliah NM, Singh H, Raj R, Surappa MK. Processing, microstructural evolution and strength properties of in-situ magnesium matrix composites containing nano-sized polymer derived SiCNO particles. Mater Sci Eng A 2017;685:429–38. https://doi.org/10.1016/j.msea.2017.01.001.
[162] Sudhagar S, Gopal PM, Maniyarasan M, Suresh S, Kavimani V. Multi-objective optimization of machining parameters for Si3N4–BN reinforced magnesium composite in wire electrical discharge machining. Int J Interact Des Manuf 2024. https://doi.org/10.1007/s12008-024-01777-3.
[163] Suresh S, Velmurugan D, Balaji J, Natarajan E, Suresh P, Rajesh S. Influences of nanoparticles in friction stir welding processes. Sustain. Util. Nanoparticles Nanofluids Eng. Appl., IGI Global 2023:32–55. https://doi.org/10.4018/978-1-6684-9135-5.ch002.
[164] Raja S, Muhamad MR, Jamaludin MF, Yusof F. A review on nanomaterials reinforcement in friction stir welding. J Mater Res Technol 2020;9:16459–87. https://doi.org/10.1016/j.jmrt.2020.11.072.
[165] Sharma V, Prakash U, Kumar BVM. Surface composites by friction stir processing: a review. J Mater Process Technol 2015;224:117–34. https://doi.org/10.1016/j.jmatprotec.2015.04.019.
[166] Bagheri B, Abbasi M, Abdollahzadeh A, Mirsalehi SE. Effect of second-phase particle size and presence of vibration on AZ91/SiC surface composite layer produced by FSP. Trans Nonferrous Met Soc China 2020;30:905–16. https://doi.org/10.1016/S1003-6326(20)65264-5.
[167] Faraji G, Asadi P. Characterization of AZ91/alumina nanocomposite produced by FSP. Mater Sci Eng A 2011;528:2431–40. https://doi.org/10.1016/j.msea.2010.11.065.
[168] Dadashpour M, Mostafapour A, Yeşildal R, Rouhi S. Effect of process parameter on mechanical properties and fracture behavior of AZ91C/SiO2 composite fabricated by FSP. Mater Sci Eng A 2016;655:379–87. https://doi.org/10.1016/j.msea.2015.12.103.
[169] Eivani AR, Tabatabaei F, Khavandi AR, Tajabadi M, Mehdizade M, Jafarian HR, et al. The effect of addition of hardystonite on the strength, ductility and corrosion resistance of WE43 magnesium alloy. J Mater Res Technol 2021;13:1855–65. https://doi.org/10.1016/j.jmrt.2021.05.027.
[170] Asadi P, Faraji G, Besharati MK. Producing of AZ91/SiC composite by friction stir processing (FSP). Int J Adv Manuf Technol 2010;51:247–60. https://doi.org/10.1007/s00170-010-2600-z.

[171] Qin D, Shen H, Shen Z, Chen H, Fu L. Manufacture of biodegradable magnesium alloy by high speed friction stir processing. J Manuf Process 2018;36:22–32. https://doi.org/10.1016/j.jmapro.2018.09.019.
[172] Ramaiyan S, Santhanam SKV, Muthuguru P. Effect of Scroll pin profile and tool rotational speed on mechanical properties of submerged friction stir processed AZ31B magnesium alloy. Mater Res 2018;21. https://doi.org/10.1590/1980-5373-mr-2017-0769.
[173] Asadi P, Givi MKB, Faraji G. Producing ultrafine-grained AZ91 from as-cast AZ91 by FSP. Mater Manuf Process 2010;25:1219–26. https://doi.org/10.1080/10426911003636936.
[174] Ramaiyan S, S kumar VS. Effect of the process parameters on magnesium alloy using the submerged friction stir process. Met Mater 2019;57:275–85. https://doi.org/10.4149/km_2019_4_275.
[175] Alavi Nia A, Omidvar H, Nourbakhsh SH. Investigation of the effects of thread pitch and water cooling action on the mechanical strength and microstructure of friction stir processed AZ31. Mater Des 2013;52:615–20. https://doi.org/10.1016/j.matdes.2013.05.094.
[176] Darras B, Kishta E. Submerged friction stir processing of AZ31 Magnesium alloy. Mater Des 2013;47:133–7. https://doi.org/10.1016/j.matdes.2012.12.026.
[177] Luo X, Cao G, Zhang W, Qiu C, Zhang D. Ductility improvement of an AZ61 magnesium alloy through two-pass submerged friction stir processing. Mater (Basel, Switzerland) 2017;10. https://doi.org/10.3390/ma10030253.
[178] Cao G, Zhang D, Chai F, Zhang W, Qiu C. Superplastic behavior and microstructure evolution of a fine-grained Mg–Y–Nd alloy processed by submerged friction stir processing. Mater Sci Eng A 2015;642:157–66. https://doi.org/10.1016/j.msea.2015.06.086.
[179] Chai F, Zhang DT, Li YY. Effect of rotation speeds on microstructures and tensile properties of submerged friction stir processed AZ31 magnesium alloy. Mater Res Innov 2014;18:S4–152. https://doi.org/10.1179/1432891714Z.000000000673. S4-156.
[180] Cao G, Zhang D, Zhang W, Qiu C. Microstructure evolution and mechanical properties of Mg–Nd–Y alloy in different friction stir processing conditions. J Alloys Compd 2015;636:12–9. https://doi.org/10.1016/j.jallcom.2015.02.081.
[181] Chai F, Zhang D, Li Y. Microstructures and tensile properties of submerged friction stir processed AZ91 magnesium alloy. J Magnes Alloy 2015;3:203–9. https://doi.org/10.1016/j.jma.2015.08.001.
[182] Luo XC, Zhang DT, Cao GH, Qiu C, Chen DL. Multi-pass submerged friction stir processing of AZ61 magnesium alloy: strengthening mechanisms and fracture behavior. J Mater Sci 2019;54:8640–54. https://doi.org/10.1007/s10853-018-03259-w.
[183] Chai F, Zhang D, Li Y, Zhang W. Microstructure evolution and mechanical properties of a submerged friction-stir-processed AZ91 magnesium alloy. J Mater Sci 2015;50:3212–25. https://doi.org/10.1007/s10853-015-8887-2.
[184] Iwaszko J, Kudła K. Microstructure, hardness, and wear resistance of AZ91 magnesium alloy produced by friction stir processing with air-cooling. Int J Adv Manuf Technol 2021;116:1309–23. https://doi.org/10.1007/s00170-021-07474-9.
[185] Ramaiyan S, Mani U, Chandran R, Velukkudi Santhanam SK. Optimization of corrosion behavior in submerged friction stir processed magnesium AZ31B alloy. https://doi.org/10.1115/IMECE2017-72559; 2017.
[186] Cao G, Zhang D, Chai F, Zhang W, Qiu C. High-strain-rate superplasticity in Mg–Y–Nd alloy prepared by submerged friction stir processing. Adv Eng Mater 2016;18:312–8. https://doi.org/10.1002/adem.201500221.
[187] Datong Z, Fang C, Yuanyuan L. High strain rate superplasticity of a fine-grained AZ91 magnesium alloy prepared by friction stir processing. In: Marquis F, editor. Proc. 8th Pacific Rim Int. Congr. Adv. Mater. Process. Cham: Springer International Publishing; 2016. p. 1065–71.
[188] Ammouri A, Kridli G, Ayoub G, Hamade R. Investigating the effect of cryogenic pre-cooling on the friction stir processing of AZ31B. Proc World Congr Eng 2014;2.
[189] Sankar R, Rathinasuriyan C, Vijayan R. Effect of friction stir processing on the high cycle fatigue behavior of AZ31B alloy. Mater Today Proc 2022;62:992–7. https://doi.org/10.1016/j.matpr.2022.04.253.
[190] Lee CJ, Huang JC. High strain rate superplasticity of Mg based composites fabricated by friction stir processing. Mater Trans 2006;47:2773–8. https://doi.org/10.2320/matertrans.47.2773.
[191] Rao GSP, Naik DBB. Investigating the effect of cryogenic process on a friction stir welding AZ 31 B magnesium alloy. 2015.
[192] Ramaiyan S, Chandran R, Santhanam SKV. Effect of cooling conditions on mechanical and microstructural behaviours of friction stir processed AZ31B Mg alloy. Mod Mech Eng 2017;7:144–60. https://doi.org/10.4236/mme.2017.74010.
[193] Chang C, DU X, Huang J. Producing nanograined microstructure in Mg–Al–Zn alloy by two-step friction stir processing. Scr Mater 2008;59:356–9. https://doi.org/10.1016/j.scriptamat.2008.04.003.
[194] DU X, Wu B. Using friction stir processing to produce ultrafine-grained microstructure in AZ61 magnesium alloy. Trans Nonferrous Met Soc China 2008;18:562–5. https://doi.org/10.1016/S1003-6326(08)60098-9.
[195] Ammouri A, Kridli G, Ayoub G, Hamade R. Pre-cooling Effects on the Resulting Grain Size in Friction Stir Processing of AZ31B 2015:355–65. https://doi.org/10.1007/978-94-017-9804-4_24.
[196] Mohammed A. Achieving ultrafine grains in Mg AZ31B-O alloy by cryogenic friction stir processing and machining. Theses Diss Syst Eng n.d.
[197] Mosayebi M, Zarei-Hanzaki A, Abedi HR, Barabi A, Jalali MS, Ghaderi A, et al. The correlation between the recrystallization texture and subsequent isothermal grain growth in a friction stir processed rare earth containing magnesium alloy. Mater Charact 2020;163:110236. https://doi.org/10.1016/j.matchar.2020.110236.
[198] Xu N, Song Q, Bao Y, Fujii H. Investigation on microstructure and mechanical properties of cold source assistant friction stir processed AZ31B magnesium alloy. Mater Sci Eng A 2019;761:138027. https://doi.org/10.1016/j.msea.2019.138027.
[199] Chandran R, Duke M, Ramaiyan S, S kumar VS. Experimental investigation of cooling medium on submerged friction stir processed AZ31 magnesium alloy. Mater Today Proc 2021;46. https://doi.org/10.1016/j.matpr.2020.11.575.
[200] Bhojak V, Jain JK, Singhal TS, Saxena KK, Prakash C, Agrawal MK, et al. Friction stir processing and cladding: an innovative surface engineering technique to tailor magnesium-based alloys for biomedical implants. Surf Rev Lett 2023. https://doi.org/10.1142/S0218625X23400073.
[201] Kundu S, Thakur L. An investigation on the fabrication and characterization of friction stir processed nano-HAp reinforced AZ91D magnesium matrix surface composite for bio-implants. J Mech Behav Biomed Mater 2023;143:105918. https://doi.org/10.1016/j.jmbbm.2023.105918.
[202] Yousefpour F, Jamaati R, Aval HJ. Synergistic effects of hybrid (HA+Ag) particles and friction stir processing in the design of a high-strength magnesium matrix bio-nano composite with an appropriate texture for biomedical applications. J Mech Behav Biomed Mater 2022;125:104983. https://doi.org/10.1016/j.jmbbm.2021.104983.
[203] Esmaeilzadeh O, Eivani AR, Mehdizade M, Boutorabi SMA, Masoudpanah SM. An investigation of microstructural background for improved corrosion resistance of WE43 magnesium-based composites with ZnO and Cu/ZnO additions. J Alloys Compd 2022;908:164437. https://doi.org/10.1016/j.jallcom.2022.164437.
[204] Mehdizade M, Eivani AR, Tabatabaei F, Mousavi Anijdan SH, Jafarian HR. Enhanced in-vitro biodegradation, bioactivity, and mechanical properties of Mg-based biocomposite via addition of calcium-silicate-based bioceramic through friction stir processing as resorbable temporary bone implant. J Mater Res Technol 2023;26:4007–23. https://doi.org/10.1016/j.jmrt.2023.08.128.
[205] Rokkala U, Jana A, Bontha S, Ramesh MR, Balla VK. Comparative investigation of coating and friction stir processing on Mg-Zn-Dy alloy for improving antibacterial, bioactive and corrosion behaviour. Surf Coatings Technol 2021;425:127708. https://doi.org/10.1016/j.surfcoat.2021.127708.
[206] Yousefpour F, Jamaati R, Jamshidi Aval H. Investigation of microstructure, crystallographic texture, and mechanical behavior of magnesium-based nanocomposite fabricated via multi-pass FSP for biomedical applications. J Mech Behav Biomed Mater 2022;125:104894. https://doi.org/10.1016/j.jmbbm.2021.104894.
[207] Eivani AR, Mehdizade M, Ghosh M, Jafarian HR. The effect of multi-pass friction stir processing on microstructure, mechanical properties, and corrosion behavior of WE43-nHA bio-composite. J Mater Res Technol 2023;22:776–94. https://doi.org/10.1016/j.jmrt.2022.11.141.
[208] thakur A, Mohammad Akram S, Waseem SKM, Kanojiya S, Gupta LR, Wandra R. Development of Mg-based biodegradable composite using friction stir processing for orthopedic application. Mater Today Proc 2022;50:684–91. https://doi.org/10.1016/j.matpr.2021.04.475.
[209] Suresh S, Kumar P, Yuvaraj T, Velmurugan D, Natarajan E. 4 Adoptability of additive manufacturing process: design perceptive. In: Kumar A, Kumar P, Sharma N, Srivastava AK, editors. Print. Technol. Berlin, Boston: De Gruyter; 2024. p. 77–94. https://doi.org/10.1515/9783111215112-004.
[210] Suresh S, Natarajan E, Boopathi S, Kumar P. 8 Processing of smart materials by additive manufacturing and 4D printing. In: Kumar A, Kumar P, Sharma N, Srivastava AK, editors. 3D Print. Technol. Berlin, Boston: De Gruyter; 2024. p. 181–96. https://doi.org/10.1515/9783111215112-008.
[211] Chen H, Meng X, Chen J, Xie Y, Wang J, Sun S, et al. Wire-based friction stir additive manufacturing. Addit Manuf 2023;70:103557. https://doi.org/10.1016/j.addma.2023.103557.
[212] Chen H, Chen J, Meng X, Xie Y, Huang Y, Xu S, et al. Wire-based friction stir additive manufacturing toward field repairing. Weld J 2022;101:249–52. https://doi.org/10.29391/2022.101.019.
[213] Das AK. Recent trends in laser cladding and alloying on magnesium alloys: a review. Mater Today Proc 2022;51:723–7. https://doi.org/10.1016/j.matpr.2021.06.217.
[214] Ahmadi M, Tabary SAAB, Rahmatabadi D, Ebrahimi MS, Abrinia K, Hashemi R. Review of selective laser melting of magnesium alloys: advantages, microstructure and mechanical characterizations, defects, challenges, and applications. J Mater Res Technol 2022;19:1537–62. https://doi.org/10.1016/j.jmrt.2022.05.102.
[215] Motallebi R, Savaedi Z, Mirzadeh H. Post-processing heat treatment of lightweight magnesium alloys fabricated by additive manufacturing: a review. J Mater Res Technol 2022;20:1873–92. https://doi.org/10.1016/j.jmrt.2022.07.154.
[216] Perry MEJ, Griffiths RJ, Garcia D, Sietins JM, Zhu Y, Yu HZ. Morphological and microstructural investigation of the non-planar interface formed in solid-state metal additive manufacturing by additive friction stir deposition. Addit Manuf 2020;35:101293. https://doi.org/10.1016/j.addma.2020.101293.
[217] Phillips BJ, Williamson CJ, Kinser RP, Jordon JB, Doherty KJ, Allison PG. Microstructural and mechanical characterization of additive friction stir-deposition of aluminum alloy 5083 effect of Lubrication on material Anisotropy. Materials 2021;14:6732. https://doi.org/10.3390/ma14216732.
[218] Farabi E, Babaniaris S, Barnett MR, Fabijanic DM. Microstructure and mechanical properties of Ti6Al4V alloys fabricated by additive friction stir deposition. Addit Manuf Lett 2022;2:100034. https://doi.org/10.1016/j.addlet.2022.100034.

[219] Soujon M, Kallien Z, Roos A, Zeller-Plumhoff B, Klusemann B. Fundamental study of multi-track friction surfacing deposits for dissimilar aluminum alloys with application to additive manufacturing. Mater Des 2022;219:110786. https://doi.org/10.1016/j.matdes.2022.110786.
[220] Griffiths RJ, Garcia D, Song J, Vasudevan VK, Steiner MA, Cai W, et al. Solid-state additive manufacturing of aluminum and copper using additive friction stir deposition: process-microstructure linkages. Materialia 2021;15:100967. https://doi.org/10.1016/j.mtla.2020.100967.
[221] Chaudhary B, Jain NK, Murugesan J, Patel V. Exploring temperature-controlled friction stir powder additive manufacturing process for multi-layer deposition of aluminum alloys. J Mater Res Technol 2022;20:260–8. https://doi.org/10.1016/j.jmrt.2022.07.049.
[222] K. Kandasamy, L. Renaghan, J.R. Calvert, K. Creehan Jps. No Title. Mater. Sci. Technol. Conf., Montreal, Qucbec, Canada: n.d., p. 27–31.
[223] Joshi SS, Patil SM, Mazumder S, Sharma S, Riley DA, Dowden S, et al. Additive friction stir deposition of AZ31B magnesium alloy. J Magnes Alloy 2022;10:2404–20. https://doi.org/10.1016/j.jma.2022.03.011.

Elango Natarajan obtained doctoral degree in Mechanical Engineering from Anna University, Chennai, India in 2010. He worked as a Post-doctoral research fellow in UTM, Skudai, Malaysia in 2013 and carried out research on soft actuators. He has served for engineering colleges/universities for about 25 years in various academic positions. He is currently attached to Faculty of Engineering, UCSI University, Malaysia as an Associate Professor. Besides, he is the Deputy Director of Praxis, Industry and Community Engagement. He has published 100+ research articles and his h-index is 21 in Scopus. He has completed many research grant projects including projects supported by Ministry of Higher Education Malaysia. He is the Chairman of IEEE Robotics and Automation Chapter Malaysia section. He is a Chartered Mechanical Engineer (CEng.) awarded by Engineering Council UK, Chartered member (CMEngNZ) awarded by Engineering Council NZ and Fellow awarded by Institution of Engineers India.

K. Palanikumar He is experienced Professor with a demonstrated history of working in the higher education industry. He is Skilled in Statistical Data Analysis, Lecturing, Curriculum Development, and Public Speaking. Strong Education Professional with a Doctor of Philosophy (PhD) focused in Department of Mechanical Engineering from Anna University, Chennai, India. He Worked Post Ph.D work on machining of Composites with Prof. J. Paulo Davim, University of Aveiro, Portugal.

He is a top 25 Scientist in materials - compiled by Stanford University, USA and World Top 1% Reviewer by Publon -Web of science Group. He is one of the International Expert in Composite Materials. He o; rganized many National and International Conferences, Technical Symposia and Faculty Development Programs. He Published more than 20 Patents and Granted 3 patents. Received Many Meritorious & Best Faculty Awards from Various Governing Bodies. Have more than 8000 citations with a h-index of 50 (Google Scholar). Also have received a grant in aid of around 1.5 crore from various funding agencies.

Dr. Prakash serving as Dean of Research & Development and Professor at Mukesh Patel School of Technology Management and Engineering, SVKM'S NarseeMonjee Institute of Management Studies, Deemed-to-be-University, Mumbai, India. He served as Dean of Research & Development/School of Mechanical Engineering at Lovely Professional University, India. He is a Ph.D. alumnus of Panjab University, Chandigarh. He is also an Adjunct Professor (Honorary position) at the Institute for Computational Science, Ton Duc Thang University, Vietnam.He is a dedicated teacher who embraces student-centric approaches, providing experiential learning to his students. He is a passionate researcher with diversified research interests-developing materials for Biomedical and Healthcare applications, additive manufacturing, and developing and exploring new cost-effective manufacturing technologies for biomedical industries. He has published over 396 (325 SCI/Scopus) scientific articles in peer-reviewed, reputable, top-notch journals, conferences, and books. Dr. Prakash is a highly cited researcher at the international level, and he has 7517 citations, an H-index of 48, and an i-10 index of 158. He is among India's Top 1% of leading Mechanical and Aerospace Engineering scientists, Research.com. He holds 38 ranks in India and 1590th rank in the world. He also consistently appeared in the top 2% of researchers as per Stanford Study in 2021, 2022, and 2023. Dr. Prakash edited/authored 25 books, serving as a Series editor of 2 books and as Guest Editor of several peer-reviewed journals.

He is an Editorial board member of Journal of Magnesium and Alloys (Elsevier, IF-17.6, SJR 2.4, Q1), Nanofabrication (IF-2.9, Q2); International Journal on Interactive Design and Manufacturing, IJIDeM (Springer, IF-2.1); Cogent Engineering (Taylor & Francis, WOS, IF: 1.9), High-Temperature Materials and Processes (De-Gruyter, IF: 1.5), Journal of Electrochemical Science and Engineering (WOS, IF: 2.1), Materials Circular Economy: Science, Engineering, and Sustainability (Springer). He is working on Research commercialisation and has published 18 patents. His 4 patents were granted. Dr. Prakash raised over 1.2 million USD in grants from various national and international bodies, including the Ministry of Science & Technology India, UKIERI-DST and SERB Government of India.

Dr.Dhanesh G. Mohan is a licensed Professional Engineer (P.E) and Chartered Engineer (C.Eng) with more than a decade of academic experience. As a Senior Lecturer in the Faculty of Technology at the University of Sunderland, United Kingdom, he oversees a research lab focusing on Net-Zero Manufacturing concepts, primarily exploring Additive Manufacturing, hybrid-TIG welding, and related fields.He is serving as an associate editor for several prestigious journals such as Part E: Journal of Process Mechanical Engineering (Sage Publishing), International Journal on Interactive Design and Manufacturing (IJIDeM) (Springer), and an academic editor for Advances in Materials Science and Engineering, and Advances in Polymer Technology (Wiley, Hindawi). Dr. Mohan is also an editorial board member for many journals, including the Journal of Adhesion Science and Technology, Taylor and Francis. In addition to his academic responsibilities, Dr. Mohan has been appointed as an Adjunct Professor at Lovely Professional University, Punjab, India. Dr. Mohan's research focuses on big-area additive manufacturing and hybrid friction stir welding methods, including Laser-assisted FSW, Ultrasonic vibration-assisted FSW, induction-assisted FSW, and FSP. His research explores the mechanical, metallurgical, corrosive, and microstructural properties of dissimilar metals and alloys such as steels, magnesium, aluminium, and high entropy alloys.

Dr. S. SURESH obtained doctoral degree in Mechanical Engineering from Anna University, Chennai, India, in 2020. Currently, he holds the position of Associate Professor in the Department of Mechanical Engineering at Erode Sengunthar Engineering College, Tamil Nadu, India. He has 12 years of teaching experience and 2 years of industry expertise in his role. His research focuses on friction stir welding of lightweight alloys and additive manufacturing.

Kiranjot Kaur currently works at Chandigarh University. Her areas of specialization are Physical Chemistry, Solution Thermodynamics, Nano Composites, and Environment. Kiranjot conducts research in Immunology, Microbiology, and Biotechnology.